



PONTIFICIA  
**UNIVERSIDAD  
CATÓLICA**  
DEL PERÚ

  
TECHNISCHE UNIVERSITÄT  
**ILMENAU**

---

# **Pontificia Universidad Católica del Perú**

Escuela de Posgrado

## **Tesis**

Implicit IDA-PBC Design and Implementation  
for a Portal Crane System

Para obtener el grado académico de:  
Magíster en Ingeniería Mecatrónica

Presentado por:    Ing. Jesus Enrique Vidal Sandoval

Tutor Responsable (TU Ilmenau):    M. Sc. Oscar B. Cieza Aguirre  
Professor Responsable (TU Ilmenau):    Prof. Dr.-Ing. Johann Reger  
Professor Responsable (PUCP):    PhD. Elizabeth Roxana Villota Cerna

Fecha y lugar:    21/10/2019, Ilmenau

# **Implicit IDA-PBC Design and Implementation for a Portal Crane System**

Master Thesis in Mechatronics / Ingeniería Mecatrónica

submitted by

**Enrique Vidal**

born on 23. October 1991  
in Lima, Peru

in the

**Control Engineering Group**

**Department of Computer Science and Automation  
Technische Universität Ilmenau**

Advisors: **Prof. Dr.-Ing. Johann Reger**  
**M. Sc. Oscar B. Cieza Aguirre**  
**PhD. Elizabeth R. Villota**

Submission Date: **21 October 2019**

## Declaration

I declare that the work is entirely my own and was produced with no assistance from third parties.

I certify that the work has not been submitted in the same or any similar form for assessment to any other examining body and all references, direct and indirect, are indicated as such and have been cited accordingly.

(Enrique Vidal)

Ilmenau, 21 October 2019

To my beloved parents  
Carmela and Enrique Vidal.

---

# Abstract

---

Interconnection and damping assignment passivity-based control (IDA-PBC) is a well-known technique which regulates the behavior of nonlinear systems, assigning a target port-Hamiltonian (pH) structure to the closed-loop. In underactuated mechanical systems (UMSs) its application requires the satisfaction of matching conditions, which in many cases demands to solve partial differential equations (PDEs). Only recently, the IDA-PBC has been extended to UMSs modeled implicitly, where the system dynamics in pH representation are described by a set of differential-algebraic equations (DAEs). In some system classes this implicit approach allows to circumvent the PDE problem and also to design an output-feedback law.

The present thesis deals with the design and implementation of the total energy shaping implicit IDA-PBC on a portal crane system located at the laboratory of the Control Engineering Group at TU-Ilmenau. The implicit controller is additionally compared with a simplified (explicit) IDA-PBC [1]. This algorithm shapes the total energy and avoids the PDE problem. However, this thesis reveals a significant implementation flaw in the algorithm, which then could be solved.

---

# Kurzfassung

---

Interconnection and damping assignment passivity-based control (IDA-PBC) ist eine wohlbekannt Methode zur Regelung von nichtlinearen Systemen, die im geschlossenen Regelkreis eine gewünschte Port-Hamiltonian-Struktur (pH) haben. Die Anwendung auf unteraktuierte mechanische Systeme (UMS) erfordert die Erfüllung von sogenannten Matching Conditions, die meistens die Lösung partieller Differentialgleichungen (PDE) benötigt. Erst kürzlich wurde die IDA-PBC auf implizit modellierte UMS erweitert, bei denen die Systemdynamik in pH-Darstellungen durch Differentialalgebraische Gleichungen (DAE) beschrieben wird. Dieser implizite Ansatz ermöglicht bei einigen Systemklassen, das PDE-Problem zu umgehen und auch eine Ausgangsrückführung zu entwerfen.

Die vorliegende Masterarbeit beschäftigt sich mit dem Entwurf und der Implementierung des impliziten IDA-PBC zur Gesamtenergievorgabe auf einem Portalkransystem im Labor des Fachgebiets Regelungstechnik der TU-Ilmenau. Der implizite Regler wird mit einem vereinfachten (expliziten) IDA-PBC verglichen [1]. Dieser Algorithmus gibt ebenso die Gesamtenergie vor und vermeidet das PDE-Problem. In der Masterarbeit wird in diesem Algorithmus ein wesentlicher Implementierungsfehler offengelegt und behoben.

---

# Acknowledgment

---

I would like to thank all the people who support me during the development of this thesis. Specially thanks are (i) to my entire family who motivated me to finish this work, (ii) to my thesis advisor M.Sc. Oscar Cieza at TU Ilmenau, he was always available to guide me in the right direction, (iii) to the responsible of the Control Engineering Group Laboratory, Axel Fink, who support me in the well use of the Equipment, and (iv) to my closest friends.

---

# Contents

---

<b>Abstract</b>	<b>iv</b>
<b>Kurzfassung</b>	<b>v</b>
<b>Contents</b>	<b>vii</b>
<b>1. Introduction</b>	<b>1</b>
1.1. Motivation . . . . .	1
1.2. Literature Review . . . . .	2
1.2.1. Portal Crane . . . . .	2
1.2.2. Common Algorithms used in Portal Crane control . . . . .	2
1.2.3. Passivity Based Control (PBC) applied to Portal Cranes . . . . .	4
1.2.4. Implicit PBC . . . . .	5
1.3. Contribution of this thesis . . . . .	6
1.4. Outline of this thesis . . . . .	6
<b>2. Theoretical Fundamentals</b>	<b>7</b>
2.1. Analytical Mechanics . . . . .	7
2.1.1. Lagrangian Mechanics . . . . .	7
2.1.1.1. Kinematics . . . . .	7
2.1.1.2. Newton's Law . . . . .	8
2.1.1.3. Generalized Coordinates . . . . .	8
2.1.1.4. Virtual Displacement . . . . .	9
2.1.1.5. Euler-Lagrange Equations . . . . .	10
2.1.1.6. The Functional and Hamilton's Principle . . . . .	10
2.1.1.7. Constraints . . . . .	11
2.1.1.8. Method of Lagrange Undetermined Multipliers . . . . .	11
2.1.1.9. Canonical Momentum . . . . .	11



2.1.2. Hamiltonian Mechanics . . . . .	11
2.1.2.1. Legendre Transformation . . . . .	12
2.1.2.2. The Hamiltonian . . . . .	12
2.1.2.3. The Canonical Equations . . . . .	13
2.1.2.4. The Hamiltonian Function with Constraints . . . . .	14
2.2. Passivity-based control and Energy Shaping . . . . .	14
2.2.1. Dissipativity, passivity and stability . . . . .	14
2.2.2. Port Hamiltonian Systems . . . . .	17
2.2.3. Implicit and Explicit Port Hamiltonian Structure of a Mechanical System . . . . .	18
2.2.4. Underactuated Mechanical Systems . . . . .	19
2.2.5. Interconnection and Damping Assignment - PBC . . . . .	19
<b>3. Implicit IDA-PBC for UMS</b>	<b>24</b>
3.1. Problem formulation . . . . .	24
3.2. Implicit Interconnection and Damping Assignment - Passivity-Based Control (IDA-PBC) for holonomic systems . . . . .	25
3.2.1. Mechanical systems with constant mass matrix . . . . .	29
3.2.2. Position feedback . . . . .	32
<b>4. Explicit and Implicit IDA-PBC applied to a Portal Crane</b>	<b>34</b>
4.1. The Portal Crane System . . . . .	34
4.1.1. Additional Information of the Crane . . . . .	36
4.1.2. 2-D Explicit Model . . . . .	37
4.1.3. 3-D Implicit Model . . . . .	39
4.2. Explicit IDA-PBC Applied to the Portal Crane . . . . .	41
4.2.1. State feedback law from [1] . . . . .	41
4.2.2. A well-defined state feedback law using IDA-PBC . . . . .	43
4.2.3. Results . . . . .	45
4.3. Implicit IDA-PBC Applied to the Portal Crane . . . . .	46
4.3.1. State feedback law . . . . .	47
4.3.2. An output feedback law using the implicit IDA-PBC approach . . . . .	49
4.3.3. Results . . . . .	49
<b>5. Conclusions and Future Work</b>	<b>57</b>
<b>Appendices</b>	<b>59</b>
<b>A. Euler-Lagrange Equations</b>	<b>60</b>

## *CONTENTS*

---

<b>Abbreviations</b>	<b>64</b>
<b>List of Figures</b>	<b>65</b>
<b>List of Tables</b>	<b>67</b>
<b>Bibliography</b>	<b>68</b>

---

# Chapter 1

## Introduction

---

### 1.1 Motivation

Underactuated Mechanical Systems (UMSs) are widely used in different scenarios in the industry, such as construction, robotic applications, and transportation. A mechanical system is said to be underactuated if it has fewer control inputs than Degrees of Freedom (DOF). The underactuation can come from different situations, such as intentional design or due to the failure of some actuators [2]. For this reason, the focus on developing new control techniques applicable to underactuated nonlinear mechanics system has grown in the last years.

At the early 2000s, classic Energy-Based Control techniques were presented to regulate the behaviour of nonlinear systems [3]. Motivated on the passivity properties of UMSs, different energy-based approaches were useful to overcome the underactuated control problem. Among them the IDA-PBC approach has been successfully used in a wide range of UMSs. The keystone of IDA-PBC is to design a closed-loop with port-Hamiltonian (pH) structure, where the new storage function has a minimum at the desired equilibrium point. However, the total energy shaping IDA-PBC has a persistent problem: the solution of Partial Differential Equations (PDEs). Recently this method has been extended theoretically to implicit pH structures [4].

The difference between an explicit model and the implicit one, relies on the considerations of physical constraints. Thus, UMSs can be modeled in explicit or implicit representation. But, if we use the implicit structure and apply the implicit IDA-PBC method, it is possible in some system classes to avoid PDEs even when the open- and closed-loop inertia mass matrices in explicit representation are state dependent. Until now, the Implicit IDA-PBC technique has remained in the theoretical and simulation framework with no physical implementation. Therefore, the main task of this master

this thesis is to apply the mentioned control algorithm on a portal crane system located at the laboratory of the Control Engineering Group at TU-Ilmenau.

## 1.2 Literature Review

### 1.2.1 Portal Crane

Cranes improve the method of transportation and handling of heavy loads. Their role in industry enables optimal throughput and logistic [5]. A crane consists of hoisting and a support mechanism. The hoisting mechanism is essentially a mechanism to lift something heavy, meanwhile, the support mechanism could be a trolley-girder, a trolley-jib, or a boom [6]. According to the degrees of freedom of the support mechanism, cranes can be classified as:

- **Rotary cranes:** They are also known as tower cranes, and here, the girder<sup>1</sup> rotates in a plane parallel to the ground about a fixed vertical axis. In Figure 1.1a we can see a rotary crane model Potain MDT 98 [7].
- **Boom cranes:** Their suspension point is fixed at the end of the boom. The main advantage relies on their structure capable of supporting loads in compression. As a result, booms are compact and offer the same capacity as the rotary cranes [6]. Figure 1.1b is a boom crane developed by [8].
- **Portal cranes:** Also known as a gantry or overhead crane. It is composed of a trolley moving over a girder, and it usually has a setup that allows the movement of the trolley on a plane parallel to the ground. Figure 1.1c shows a Rubber-Tyred Gantry Crane Terex by [9].

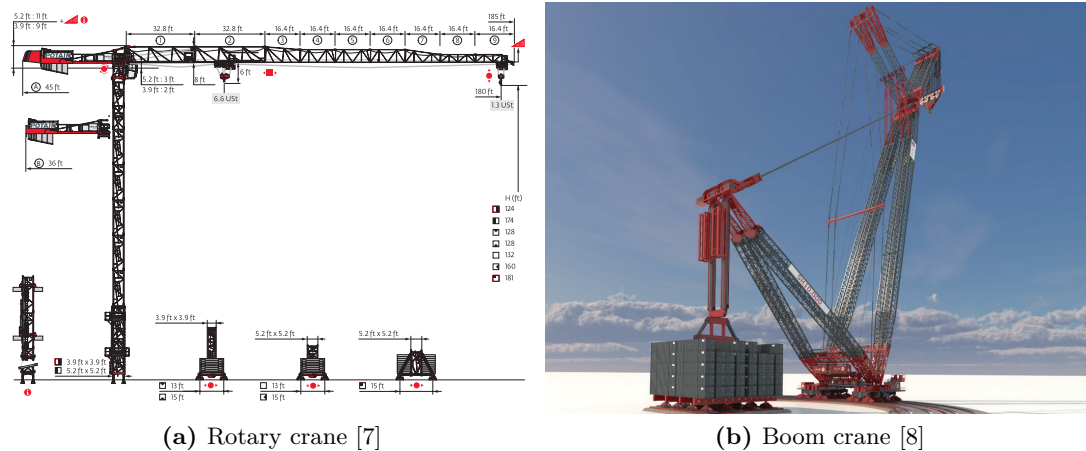
There exists two main approaches to model a crane, the distributed mass model and the lumped mass model. The first considers the hoisting line as a distributed mass, hence the name [10], while the latter considers the hoisting line as a massless cable. In this thesis, we use the lumped-mass model and consider the cable-hook-payload as a spherical pendulum.

### 1.2.2 Common Algorithms used in Portal Crane control

Moving a load from one position to another is an essential task of any crane. However, an inadequate control in the actuators will increase oscillations on the payload. Considering that it will move a heavy load, requiring safe movements to protect the workers

---

<sup>1</sup>A girder is a long, thick piece of metal. Normally, the frame of the cranes is composed of a set of girders.



(c) Gantry crane [9]

**Figure 1.1.** – Different kind of cranes

and objects in the workspace. In this sense, it is desired to have minimal residual pendulations en route to the target destination. A primitive idea will be to perform the motion with minimum velocity. However, this leads in wasting time and thus, lacking in efficiency and efficacy.

In [6], a detailed survey of the earliest controllers applied to cranes is presented. The author describes different open and closed loops techniques including linear control, fuzzy control, optimal control, adaptive control and nonlinear control. Here, we described some of the most relevant nonlinear control approaches:

*Sliding mode control (SMC).* In [11] the author models the crane dynamics in 3-D and proposes two clear objectives: position regulation and anti-swing control. Besides, it is

implemented an observer contemplating that most of the cranes are not equipped with velocity sensors. The results of the simulations confirm that using SMC increments the robustness under uncertain parameters. In [12] the method is extended to Second-order sliding mode control (SOSMC). The author proposes a SOSMC controller for a 3-D crane affected by external perturbations. The work seeks a strong Lyapunov function to enable the use of the twisting algorithm; and, SMC enforcement to deal with uncertainties and initial swing angle conditions. An extension to Adaptive Dynamic SMC was presented in [13]. That work proposes to eliminate the effect of chattering caused by SMC through a dynamic integral sliding surface. An advantage of this approach is the self-tuning laws which overcome the disturbances and uncertainties. However, the model is restricted to 2-D.

*Partial Feedback Linearization (PFL).* In [14] the author uses the PFL combined with  $H_\infty$  control theory applied to a 3-D crane model. The approach explores two scenarios: system without movement and with external perturbations, and trajectory tracking. The results are implemented in a real system and compared with pole placement and LQR approach.  $H_\infty$  and  $H_\infty$  loop-shaping control show a robustification and good performance.

### 1.2.3 PBC applied to Portal Cranes

In this subsection, we describe some of the classic energy-based control techniques in portal crane systems. All of them assume the lumped mass model:

*Interconnection and Damping Assignment - Passivity-Based Control (IDA-PBC).* In [15] the authors analyze the crane in 2-D with a holonomic constraint and apply the potential energy shaping IDA-PBC.<sup>2</sup> The main idea is to assign the closed-loop dynamics a desired Hamiltonian and solve the matching conditions to obtain a nonlinear control law. Here the authors take as the holonomic constraint a no-slip restriction in the pulley/cable model and their controller achieves (local) asymptotic stability.

In [1, 16] it is used a Simplified IDA-PBC approach. The paper follows the procedure of IDA-PBC with a particular parametrization in the closed-loop inertia matrix, enabling a kinetic energy shaping and a simplification in the PDEs of the matching conditions. The work considers a 2-D crane model under partial feedback linearization. However, the controller has a division by 0 problem in some points or regions of the state space, e.g. if the system begins at equilibrium. In [17] the author applies a Combined Flatness and IDA-PBC approach. They develop a point-to-point transfer of the payload minimizing the cable swing. The crane model is in 2-D and considers holonomic constraints analyzing the pulley/cable. Besides, they achieve a trajectory

---

<sup>2</sup>The total energy shaping IDA-PBC methodology will be explained in Section 2.2.5.

tracking using flatness and considering feedforward control based on flatness. They find a lack of robustness due to the open-loop nature of flatness based feedforward control and add the IDA-PBC methodology (solving a PDE) to stabilize the system.

*Energy Shaped without solving the PDE.* In [18] the authors propose a control law in two stages. The first stage uses the collocated partial feedback linearization method, and the second stage is a PI Controller. The technique follows a problem formulation using a Hamiltonian energy function but does not impose a mechanical pH structure in the closed-loop. Additionally, they use (Cyclo) passive outputs and consider the model of the crane in 2-D. Unfortunately, the paper does not show simulations or a physical implementation.

*Geometric-PBC.* In [19] the authors take advantage of the intrinsic geometry of a 3-D underactuated crane with 4-DOF. They use PFL and new passivating outputs to shape only the potential energy. Finally, they obtain a nonlinear control law without solving PDEs.

#### 1.2.4 Implicit PBC

The implicit representation has its root in analytical mechanics, where remarkable contributions of this theory were the Euler-Lagrange equations introduced in 1788, the Hamilton contributions presented in two essays 1834 and 1835 [20], and also the Jacobi Contributions of 1837, well-known as the Hamilton-Jacobi method [21]. In [22], the authors explore the explicit and implicit representations of smooth, finite-dimensional pH systems. They explain briefly the conditions to model a system in implicit representation, i.e., due to physical constraints.

*PBC of pH systems* [3]. This work is one of the main contributions to PBC with Dirac structure. Here, the energy balancing PBC, the control by state-modulated source, and the IDA-PBC methodology, are generalized to the case in which the system is model from a Dirac-structure perspective. The author focus on electrical circuits.

*Implicit IDA-PBC for UMS* [4]. The work presents a generalization of IDA-PBC to UMS described in implicit pH representation. The paper exposes a state-feedback and output-feedback law using a similar procedure as in (explicit) algebraic IDA-PBC. Thus, the main contributions of this work are the solution of the IDA-PBC method for UMS with holonomic constraints and avoiding PDEs. As an example of the proposed approach, a 3-D model of the crane with holonomic constraints was taken into consideration. The simulations of the output-feedback control law without using partial feedback linearization shows an (local) asymptotical response.

### **1.3 Contribution of this thesis**

This master thesis briefly reviews the theory of implicit IDA-PBC for UMS with holonomic constraints. Then, the implicit algorithm is designed, simulated and then implemented in a portal crane system located at the laboratory of the Control Engineering Group at TU-Ilmenau. The model considered for the implicit IDA-PBC is in 3-D with the constraint given by a fix pendulum cable length. This work uses a computer with MATLAB/SIMULINK and an RTI toolbox which enables rapid prototyping in the implementation thanks to the dSPACE controller board. For comparison, it is also designed the (explicit) IDA-PBC algorithm to the portal crane modeled in 2-D and, revealing a significant mistake made by [1]. The (local) asymptotic stability of the system is investigated through simulations and implementations that were carried out and finally compared.

### **1.4 Outline of this thesis**

The remainder of the thesis is organized as follows: Chapter 2 gives an overview of the theoretical fundamentals required to understand the implicit IDA-PBC. It includes the essential background for explicit and implicit port Hamiltonian (pH) modeling of mechanical systems, and a concise introduction to passivity based control (PBC) and IDA-PBC. Chapter 3 briefly provides the theory of IDA-PBC for implicit systems. In Chapter 4, focused on the portal crane, the design is presented, also simulations and real implementation for both explicit and implicit IDA-PBC algorithms. This thesis concludes in Chapter 5 with a summary of the most important remarks and ideas for future work.



---

## Chapter 2

# Theoretical Fundamentals

---

This chapter presents the theoretical basis, which this thesis is built on. After some brief mathematical preliminaries based on the authors of [23–25], we introduce simple mechanical systems in both Lagrangian and Hamiltonian representations in Section 2.1.1 and Section 2.1.2, respectively. We then recall some notions of passivity and passivity-based control theory in Section 2.2.

### 2.1 Analytical Mechanics

In essence, Analytical Mechanics is the theory on which we base our understanding of motion [23]. A vast number of mathematicians have contributed to the theory of Analytical Mechanics, for example, Copernicus, Kepler, Newton, D’Alembert, Euler, Lagrange, Hamilton and Jacobi. From them we might distinguish Lagrange and Hamilton, which are the fathers of Lagrangian and Hamiltonian Mechanics. In this work, we repeatedly talk about explicit<sup>3</sup> and implicit port Hamiltonian (pH) representations, but to understand both, we recall Lagrange and Hamiltonian Mechanics.

#### 2.1.1 Lagrangian Mechanics

##### 2.1.1.1 Kinematics

Kinematics is the description of the motion of particles. Commonly, those particles are called point particles which, in classical mechanics, means that are small enough compared to the dimensions of the system. The motion of a system consists of a collection of  $n$  point particles with masses  $m_i$ ,  $i = \{1, 2, \dots, n\}$ . In order to define the kinematic description of a particle, i.e., to recognize a position vector and a velocity vector, we might choose Cartesian coordinates as in Figure 2.1. Here the vector position

---

<sup>3</sup>For simplicity, most authors omit the word *explicit* when referring to explicit pH systems.

is  $\mathbf{r} \in \mathbb{R}^n$  and  $\mathbf{r} = \mathbf{r}(t) = (\mathbf{x}(t), \mathbf{y}(t), \mathbf{z}(t))$ . The length from the origin to the vector is defined by the Euclidean Norm  $\|\mathbf{r}\|_2$ . Besides, because only the components  $(\mathbf{x}, \mathbf{y}, \mathbf{z})$  are time dependent, the velocity vector  $\mathbf{v} \in \mathbb{R}^n$  is  $\mathbf{v}(t) := d\mathbf{r}/dt \equiv \dot{\mathbf{r}}$ . Similarly, the acceleration vector  $\mathbf{a} \in \mathbb{R}^n$  is  $\mathbf{a}(t) := d\dot{\mathbf{r}}/dt \equiv \ddot{\mathbf{r}}$ .

### 2.1.1.2 Newton's Law

The total force acting on the  $i^{th}$  (point) particle is defined by  $\mathbf{F}_i = \mathbf{F}_i^{ext} + \mathbf{F}_i^{int}$ . Where  $\mathbf{F}_i^{ext}$  and  $\mathbf{F}_i^{int}$  are the external and internal forces respectively. Applying Newton's Second Law to our Cartesian coordinates  $(x,y,z)$ , results in a set of three equations, which we may sum over all particles  $i$  to obtain

$$\sum_{i=1}^n m_i \ddot{\mathbf{r}}_i = \sum_{i=1}^n \mathbf{F}_i. \quad (2.1)$$

### 2.1.1.3 Generalized Coordinates

Geometric constraints are normally imposed due to physical constraints on the system. Leading in the possibility of achieving the complete description of the motion in terms of some dynamical variables. As an example, consider the simple pendulum in Figure 2.2 where the motion of the mass is constrained to follow the path of a circle of radius  $l$ . The Cartesian coordinates of the system are  $x = l \sin \beta$  and  $z = l \cos \beta$ . Thus, the description of the motion is in terms of a single variable  $\beta$ . This variable expresses the relationship between  $x$  and  $y$ , and we refer to this variable as the generalized coordinate. In this particular case, the reduction of coordinates results from the single constraint  $l^2 = x^2 + y^2$ .

Let us define the generalized coordinates  $\mathbf{q} \in \mathbb{R}^{n_q}$  and an element of this set as  $q_k$ , where  $k = 1 \dots n_q$ . Besides,  $1 \leq n_q \leq N$  and  $N$  is an integer number indicating the number of degrees of freedom. Thus,

$$\{\mathbf{r}_1, \mathbf{r}_2, \dots, \mathbf{r}_n\} \rightarrow \{q_1, q_2, \dots, q_{n_q}\}. \quad (2.2)$$

To formulate a general case, where the generalized coordinates and the constraints of the system are together, it will require the method of undetermined multipliers introduced by Lagrange and later explained in Section 2.1.1.8. From the pendulum example, it is clear that constraints will always impose geometrical relationships between the rectangular coordinates  $\mathbf{r}$  and the generalized coordinates  $\mathbf{q}$ . Is common to represent

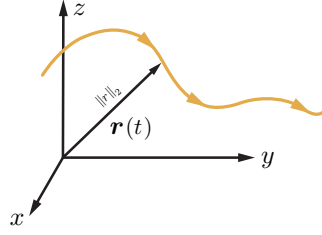


Figure 2.1. – Rectangular Cartesian Coordinates

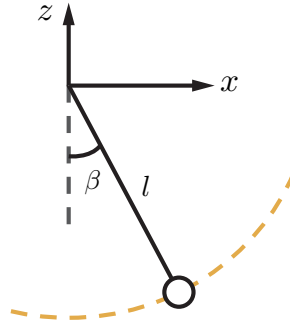


Figure 2.2. – Pendulum with generalized coordinate  $\beta$

this relationship as

$$\mathbf{r}_i = \mathbf{r}_i(q_1, q_2, \dots, q_{n_q}, t) = \mathbf{r}_i(\mathbf{q}, t); \quad i = 1, \dots, n. \quad (2.3)$$

From above equation we can write

$$\mathbf{v}_i \equiv \frac{d\mathbf{r}_i}{dt} = \sum_{k=1}^{n_q} \frac{\partial \mathbf{r}_i}{\partial q_k} \dot{q}_k + \frac{\partial \mathbf{r}_i}{\partial t}, \quad (2.4)$$

which is usually called Pfaffians or Pfaff's differential forms.

#### 2.1.1.4 Virtual Displacement

The virtual displacement  $\delta \mathbf{r}_i$  is a purely imaginary movement along the path of the particles. It is called virtual since it does not actually happen. The central assumption for virtual displacement is that the time is constant and thus  $dt = 0$ . From (2.4), with  $dt = 0$ , we have

$$\delta \mathbf{r}_i = \sum_{k=1}^{n_q} \frac{\partial \mathbf{r}_i}{\partial q_k} \delta q_k. \quad (2.5)$$

### 2.1.1.5 Euler-Lagrange Equations

A derivation from d'Alembert's Principle (see Appendix A) will lead to the well known Euler-Lagrange equation

$$\frac{\partial L}{\partial q_k} - \frac{d}{dt} \left( \frac{\partial L}{\partial \dot{q}_k} \right) = 0, \quad (2.6)$$

$$L(q, \dot{q}, t) = T - V, \quad (2.7)$$

where  $L$  is the Lagrangian,  $T$  is the kinetic energy and  $V$  represents the potential energy.

### 2.1.1.6 The Functional and Hamilton's Principle

A functional defines an operation on a class of functions  $\{y(x)\}$  that returns a real number for each function  $y(x)$  [23]. The functional is typically denoted as  $J[y]$  and it typically has the following form

$$J[y] = \int_a^b F(y(x), y', x) dx \quad \text{with} \quad y' = \frac{d}{dx} y(x). \quad (2.8)$$

Here the functional is a definite integral of a quantity  $F$  dependent on the function  $y(x)$ , its derivative  $y'(x)$ , and the independent variable  $x$  over the interval  $[a, b]$ .

**Theorem 1** (Hamilton's Principle [23]). *Let  $S[q]$  be a functional*

$$S[q] = \int_{t_1}^{t_2} L(q, \dot{q}, t) dt,$$

where  $L$ , defined in (2.7), is the Lagrangian function with generalized coordinates  $q \in \mathbb{R}^{n_q}$ , which have continuous first time derivatives  $\dot{q}$  on the interval  $[t_1, t_2]$ , and fixed values at the end points  $t_1$  and  $t_2$ . Then a necessary condition for  $S[q]$  to have an extremum for a given set of generalized coordinates  $q$  is that each generalized coordinate  $q$  satisfies the Euler-Lagrange Equation

$$\frac{\partial L}{\partial q_k} - \frac{d}{dt} \left( \frac{\partial L}{\partial \dot{q}_k} \right) = 0 \quad k = 1, \dots, n_q$$

.

### 2.1.1.7 Constraints

We might reduce the number of generalized coordinates through constraints imposed on the system. There are different kinds of constraints; however, this thesis focuses on the holonomic constraints, i.e, constraints that we can write algebraically as

$$\mathbf{g}(q) = 0. \tag{2.9}$$

### 2.1.1.8 Method of Lagrange Undetermined Multipliers

The method of Lagrange undetermined multipliers consists in incorporate the constraints (2.9) to the system. This method defines  $\boldsymbol{\lambda} \in \mathbb{R}^{n_\lambda}$  arbitrary functions of time, which yield  $n_\lambda$  equations

$$\lambda_k g_k = 0. \tag{2.10}$$

Incorporating the integral of the products of Equation (2.10) to the functional in the Theorem 1 (Hamilton's Principle) leads to an 'augmented' Lagrangian  $L' = L + \sum_{k=1}^{n_\lambda} \lambda_k g_k$ . Theorem 1 then results in the modified Euler-Lagrange equations

$$\frac{\partial L}{\partial q_k} - \frac{d}{dt} \left( \frac{\partial L}{\partial \dot{q}_k} \right) + \sum_{k=1}^{n_\lambda} \lambda_k \frac{\partial g_k}{\partial q_k} = 0. \tag{2.11}$$

### 2.1.1.9 Canonical Momentum

The canonical momenta  $\mathbf{p}$  that conjugate to the generalized coordinates  $\mathbf{q}$  are defined as

$$p_k \equiv \frac{\partial L}{\partial \dot{q}_k}. \tag{2.12}$$

For a free particle the momentum that conjugates with  $x$  is  $p = m\dot{x}$ , and thus canonically conjugate momentum reduces to the usual definition of momentum [24] which is well known in classical mechanics as linear momentum [26].

## 2.1.2 Hamiltonian Mechanics

We can represent the system dynamics described by the Euler-Lagrange equations in an utterly equivalent form called the Hamiltonian. This section shows that the Lagrangian will have a transition from a formulation on a single second-order Euler-Lagrange equation to one based on two first-order equations, one for each generalized coordinate and one for each conjugate momentum. To achieve this transition we need to perform a Legendre transformation. Then, we find the fundamental equations of Analytical Mechanics which are well know as the canonical equations.

### 2.1.2.1 Legendre Transformation

The Legendre transformation is a very useful mathematical tool since it transforms functions on a vector space to functions on the dual space. Legendre transformations are also related to projective duality and tangential coordinates in algebraic geometry. Formal definitions of this transformation can be found in [25] and in Appendix C of [27]. But, to have a general overview we follow the explanation in [23]. Consider a function of two variables  $\Psi(\xi, \eta)$  and consider a new variable  $\zeta$  such that

$$\zeta = \frac{\partial \Psi}{\partial \eta}. \quad (2.13)$$

Now represent  $\Psi$  in Pfaff form, i.e.,

$$d\Psi = \frac{\partial \Psi}{\partial \xi} d\xi + \frac{\partial \Psi}{\partial \eta} d\eta. \quad (2.14)$$

If we define  $\Phi := \eta \zeta - \Psi$ , and replace Equations (2.13) and (2.14) in its differential, we obtain

$$\begin{aligned} d\Phi &= d\eta \zeta + \eta d\zeta - d\Psi \\ &= \eta d\zeta + \zeta d\eta - \frac{\partial \Psi}{\partial \xi} d\xi - \zeta d\eta \\ &= \eta d\zeta - \frac{\partial \Psi}{\partial \xi} d\xi. \end{aligned} \quad (2.15)$$

The function  $\Phi$  depends on  $(\psi, \zeta)$  rather than on  $(\psi, \eta)$ . In doing so, we have encountered the Legendre transformation.

### 2.1.2.2 The Hamiltonian

Consider the Lagrangian as  $\Psi$  and the variable  $\zeta$  as the canonical momenta  $p_j$ . Using the Legendre Transform we obtain

$$H(\mathbf{p}, \mathbf{q}, t) = \sum_k p_k \dot{q}_k - L(\mathbf{q}, \dot{\mathbf{q}}, t), \quad (2.16)$$

where  $H$  in (2.16) is called the Hamiltonian. The differential of this Hamiltonian is

$$\begin{aligned}
 dH &= \sum_k (p_k dq_k + q_k dp_k) - dL(\mathbf{q}, \dot{\mathbf{q}}, t) \\
 &= \sum_k (p_k dq_k + q_k dp_k) - \sum_k \left[ p_k dq_k + \left( \frac{\partial L}{\partial q_k} \right) dq_k \right] - \frac{\partial L}{\partial t} dt \\
 &= \sum_k \left[ - \left( \frac{\partial L}{\partial q_k} \right) dq_k + q_k dp_k \right] - \frac{\partial L}{\partial t} dt.
 \end{aligned} \tag{2.17}$$

### 2.1.2.3 The Canonical Equations

The general form of the Pfaffian of the Hamiltonian  $H(\mathbf{q}, \mathbf{p}, t)$  is

$$dH = \sum_k \left[ \left( \frac{\partial H}{\partial q_k} \right) dq_k + \left( \frac{\partial H}{\partial p_k} \right) dp_k \right] + \frac{\partial H}{\partial t} dt. \tag{2.18}$$

We can rewrite the Euler-Lagrange equations (2.6) using the canonical momentum (2.12) to obtain

$$\frac{\partial L}{\partial q_k} = \frac{d}{dt} p_k = \dot{p}_k. \tag{2.19}$$

Then, (2.17) becomes

$$dH = \sum_k [-\dot{p}_k q_k + q_k dp_k] - \frac{\partial L}{\partial t} dt. \tag{2.20}$$

Equating (2.18) and (2.20) we obtain the canonical equations of the Hamilton, that is

$$\dot{q}_k = \frac{\partial H}{\partial p_k} \quad \rightarrow \quad \dot{\mathbf{q}} = \left( \frac{\partial H}{\partial \mathbf{p}} \right)^\top, \tag{2.21}$$

and

$$\dot{p}_k = -\frac{\partial H}{\partial q_k} \quad \rightarrow \quad \dot{\mathbf{p}} = -\left( \frac{\partial H}{\partial \mathbf{q}} \right)^\top. \tag{2.22}$$

It is important to notice that the partial derivatives  $\partial H/\partial t$  and  $-\partial L/\partial t$  can not be equated since they were taken considering different variables. However, because  $dq_k/dt = \dot{q}_k$  and  $dp_k/dt = \dot{p}_k$  is feasible to evaluate  $-\partial L/\partial t$  from Equation (2.20)

$$-\frac{\partial L}{\partial t} = \frac{dH}{dt} + \sum \left[ \dot{p}_k \frac{dq_k}{dt} - \dot{q}_k \frac{dp_k}{dt} \right] = \frac{\partial H}{\partial t}. \tag{2.23}$$

The Hamiltonian is then a constant of the system motion provided the Lagrangian does not depend explicitly on the time  $t$ .

### 2.1.2.4 The Hamiltonian Function with Constraints

In Section 2.1.1.7 we consider  $\mathbf{g}(\mathbf{q}) = 0$  where  $\mathbf{g} : \mathbb{R}^{n_q} \rightarrow \mathbb{R}^{n_\lambda}$  are constraint equations and  $\boldsymbol{\lambda} \in \mathbb{R}^{n_\lambda}$  are arbitrary functions with  $\lambda_k g_k = 0$ . If we incorporate the constraints in the Hamilton's Principal Function, we obtain

$$S = \int_{t_1}^{t_2} dt \left\{ \left[ \sum_k p_k \dot{q}_k - H \right] + \sum_k \lambda_k g_k \right\}. \quad (2.24)$$

Now we can find the  $\delta$ -variation similar as in the Lagrangian Formulation, which will lead in the canonical equations with constraints, that is

$$\dot{q}_k = \frac{\partial H}{\partial p_k} \quad \rightarrow \quad \dot{\mathbf{q}} = \left( \frac{\partial H}{\partial \mathbf{p}} \right)^\top, \quad (2.25)$$

and

$$\dot{p}_k = -\frac{\partial H}{\partial q_k} + \sum_k^{n_\lambda} \lambda_k \frac{\partial g_k}{\partial q_k} \quad \rightarrow \quad \dot{\mathbf{p}} = -\left( \frac{\partial H}{\partial \mathbf{q}} \right)^\top + \left( \frac{\partial \mathbf{g}}{\partial \mathbf{q}} \right)^\top \boldsymbol{\lambda}. \quad (2.26)$$

## 2.2 Passivity-based control and Energy Shaping

The term PBC was first introduced in the context of motion control of mechanical systems [28]. The main idea is to define a controller which achieves stabilization by rendering the system passive with respect to some desired storage function and injecting damping. Energy shaping is a PBC, which has its roots in the work (Potential energy shaping) of Takegaki and Arimoto [29] long before it was related to passivity [30]. The goal of energy shaping is to virtually modify the energy of the system, composed of kinetic and potential energy, to stabilize the desired equilibrium.

In this thesis, we focus our attention on an energy shaping control method suitable for mechanical systems: Interconnection and Damping Assignment (IDA).

### 2.2.1 Dissipativity, passivity and stability

Dissipativity and Passivity properties describe the notion of energy dissipation subject to a system. The goal is to realize that a system cannot have, at a certain time, more energy than what was injected into it. To mathematically consolidate the concept we must define a storage function, i.e., how much energy is stored in the system, and a supply rate, i.e., a measure of how fast external energy is injected in the System. The mathematical basis presented here is well explained in [31–35]



**Assumption 1.** *The system*

$$\Sigma : \begin{cases} \dot{x} = f(x, u) & x(t) \in \mathcal{X} \subseteq \mathbb{R}^{n_x}, \\ y = h(x, u) & u(t) \in \mathcal{U} \subseteq \mathbb{R}^{n_u}, \\ & y(t) \in \mathcal{Y} \subseteq \mathbb{R}^{n_y}, \end{cases} \quad (2.27)$$

with  $f(0,0) = 0$  and  $h(0,0) = 0$  for all  $x(0) = x_0$  and inputs  $u = u(t)$  is the solution  $x(t) = \varphi(x_0, u(t), t)$ ,  $\forall t \geq 0$ . Where  $s : \mathcal{U} \times \mathcal{Y} \rightarrow \mathbb{R}$  is the supply rate of  $\Sigma$ , which satisfies for all  $x_0 \in \mathcal{X}$  and  $\forall u(t) \in \mathcal{U}$  the condition:

$$\int_0^t |s(u(\tau), y(\tau))| d\tau < \infty, \forall t \geq 0.$$

**Definition 1 (Dissipativity [35]).** *The system  $\Sigma$  is said to be **dissipative** with respect to the supply rate  $s$ , if there is a **non-negative storage function**  $V(x) \geq 0, V : \mathcal{X} \rightarrow \mathbb{R}^+$ , such that  $\forall x_0 \in \mathcal{X}$  and  $\forall u(t) \in \mathcal{U}$  fulfills the integral dissipation inequality (IDE)*

$$V(x(t)) - V(x_0) \leq \int_0^t s(u(t), y(t)) dt, \forall t \geq 0 \quad (2.28)$$

where  $x = \varphi(x_0, u(t), t)$ . In case the IDE becomes a equality, the system  $\Sigma$  is called *loss-free*.  $\square$

Frequently  $V$  is continuous and differentiable, then, the derivation of  $V$  along the solution  $x = x(t)$  is given by the **Differential Dissipativity Inequality (DDI)**

$$\frac{\partial V}{\partial x} f(x, u) \leq s(u(t), y(t)), \forall t \geq 0.$$

**Definition 2 (Passivity [35]).** *A system  $\Sigma$  with  $n_u = n_y$  is called **passive** if it is dissipative with respect to the supply rate  $s(u, y) = y^\top u$  and there is a storage function  $V$  satisfying  $V(0) = 0$ .  $\square$*

In the literature we can find different types of passive systems. These are shown in Table 2.1. It is important to notice that a passive system cannot store more energy than it is supplied from the outside, and a mechanical system satisfies the energy conservation, that is

$$\text{Stored energy} = \text{Supplied energy} - \text{Dissipation}$$

**Definition 3 (Zero-State observable (ZSO) [35]).** *The System  $\Sigma$  is zero-state observable if  $u(t) = 0, y(t) = 0, \forall t \geq 0$ , implies  $x(t) = 0, \forall t \geq 0$ .  $\square$*

Type of passivity	Description
Strictly passive	If there is a function $\psi(x) > 0$ such that the supply rate $s(u, y) = y^\top u - \psi(x)$ .
Strictly input passive	If there is a $\psi(x)$ with $u^\top \psi(u) > 0, \forall u \neq 0$ s.t. the supply rate $s(u, y) = y^\top u - u^\top \psi(u)$ .
$\alpha$ -input passive	If there is an $\alpha > 0$ s.t. the supply rate $s(u, y) = y^\top u - \alpha \ u(t)\ ^2$ .
strictly output passive	If there is an $S(y)$ with $y^\top S(y) > 0 \forall y \neq 0$ s.t. the supply rate $s(u, y) = y^\top u - y^\top S(y)$ .
$\beta$ -output passive	If there is a $\beta > 0$ such that the supply rate $s(u, y) = y^\top u - \beta \ y(t)\ ^2$ .
Conservative	If it is loss-free.

**Table 2.1.** – Types of passivity

A weaker version of the observability property, used to prove asymptotic stability, is presented in the next definition.

**Definition 4 (Zero-State detectable (ZSD) [35]).** *The System  $\Sigma$  is zero-state detectable if  $u(t) = 0, y(t) = 0, \forall t \geq 0$ , implies  $\lim_{t \rightarrow \infty} x(t) = 0$ .*  $\square$

**Lemma 1 (Passivity and Lyapunov Stability).** *Consider a system  $\Sigma$  with storage function  $V \in C^1$ . The equilibrium  $x = 0$  of  $\dot{x} = f(x, 0)$  is said to be asymptotically stable, if one of the two following conditions hold*

1. *The system  $\Sigma$  is strictly passive.*
2. *The system  $\Sigma$  is strictly output passive with  $V$  positive definite and ZSO.*

*In addition, if  $V$  is radially unbounded, then  $x = 0$  is globally asymptotically stable. We can extend this with two additional properties*

- (i) *If  $\Sigma$  is ZSD, then the equilibrium  $x = 0$  of  $\Sigma$  with  $u = 0$  is stable.*
- (ii) *When there is no throughput, i.e.,  $y = h(x)$ , the feedback  $u = -y$  achieves asymptotic stability of  $x = 0$  iff  $\Sigma$  is ZSD.*  $\square$

*Proof.* see [30, 36]  $\square$

**Assumption 2.** From now on, it is assumed that  $\Sigma$  has no feedthrough terms, i.e.  $y = h(x)$ .

### 2.2.2 Port Hamiltonian Systems

The class of Hamiltonian systems, i.e., the canonical equations and the Hamiltonian function, is usually related to network modelling, which extends to include Dirac structures. In simple words, a Dirac structure<sup>4</sup> is a linear space which describes internal power flows and allows the power exchange between the system and the environment via a set of input and outputs, called *ports*, giving rise to the prominent term port-Hamiltonian (pH) system. These extended models reveal the passivity properties which we can use to perform the passivity-based control laws. The mathematical concepts here presented are a brief review of [22,37,38]. We consider port-Hamiltonian systems of the form

$$\Sigma : \begin{cases} \dot{x} &= (J(x) - R(x))\left(\frac{\partial H}{\partial x}\right)^\top + G_u(x)u, & x(t) \in \mathcal{X} \subseteq \mathbb{R}^{n_x}, \\ & & u(t) \in \mathcal{U} \subseteq \mathbb{R}^{n_u}, \\ y &= h(x) := G_u^\top(x)\left(\frac{\partial H}{\partial x}\right)^\top, & y(t) \in \mathcal{Y} \subseteq \mathbb{R}^{n_u}, \end{cases} \quad (2.29)$$

where the continuously differentiable Hamiltonian function  $H : \mathcal{X} \rightarrow \mathbb{R}$  is bounded from below, and represents the stored energy  $H(x) \geq 0$  and follows the IDE. Further,  $J : \mathcal{X} \rightarrow \mathbb{R}^{n_x \times n_x}$  is the power-conserving internal interconnection structure and it is skew symmetric, that is  $J(x) = -J^\top(x)$ , and  $R : \mathcal{X} \rightarrow \mathbb{R}^{n_x \times n_x}$  is a symmetric matrix (usually called the resistive structure), which characterizes the energy dissipation, and is positive semidefinite for physical systems. The input  $u$  and the output  $y$  are conjugate variables, i.e, their product gives a power quantity. The system  $\Sigma$  with storage function  $H(x)$  is passive, because the passivity inequality

$$\begin{aligned} \dot{H} &= \frac{\partial H}{\partial x} \dot{x} \\ &= \frac{\partial H}{\partial x} \left( (J(x) - R(x))\left(\frac{\partial H}{\partial x}\right)^\top + G_u(x)u \right) \\ &= \frac{\partial H}{\partial x} J(x)\left(\frac{\partial H}{\partial x}\right)^\top - \frac{\partial H}{\partial x} R(x)\left(\frac{\partial H}{\partial x}\right)^\top + \frac{\partial H}{\partial x} G_u(x)u \\ &= -\frac{\partial H}{\partial x} R(x)\left(\frac{\partial H}{\partial x}\right)^\top + y^\top u \leq y^\top u \end{aligned} \quad (2.30)$$

holds. If  $u = 0 \rightarrow \dot{H} \leq 0$  and  $H(x)$  has an isolated minimum in  $x^*$ , i.e,  $x^* = \arg \min H$ , then  $H$  is a (weak) Lyapunov Function. Besides, if we add damping of the form

<sup>4</sup>However, in this work we use modulated Dirac structures which are not linear spaces, see [32,37].

$u = -\phi(y)$ , for a function  $\phi : \mathcal{Y} \rightarrow \mathbb{R}^{n_y}$  satisfying  $\phi(y) y > 0, \forall y \neq 0$ , then asymptotic stability (in  $x^*$ ) is guaranteed if (2.29) is zero-state detectable (ZSD).

### 2.2.3 Implicit and Explicit Port Hamiltonian Structure of a Mechanical System

In Section 2.1.1 we have seen that a mechanical system can be described by generalized coordinates  $\mathbf{q} \in \mathbb{R}^{n_q}$ . Let us represent the potential energy with  $V = V(\mathbf{q})$  and the kinetic energy in the quadratic form  $T = T(\mathbf{q}, \dot{\mathbf{q}}) = \frac{1}{2} \dot{\mathbf{q}}^\top M(\mathbf{q}) \dot{\mathbf{q}}$ , where  $M(\mathbf{q})$  is the symmetric and positive definite mass matrix. The system behavior is defined by the Lagrange equations  $\frac{d}{dt} \left( \frac{\partial L}{\partial \dot{q}_k} \right) = \frac{\partial L}{\partial q_k}$ , where the corresponding Lagrangian is  $L = T - V$ . In Section 2.1.2 we showed how Hamilton simplified the structure of the Lagrange equations by introducing the momenta  $p_k \equiv \frac{\partial L}{\partial \dot{q}_k}$  and the Hamiltonian as a function of  $\mathbf{p}$  and  $\mathbf{q}$ , i.e.  $H = H(\mathbf{p}, \mathbf{q}, \dot{\mathbf{q}})$  where  $H = \mathbf{p}^\top \dot{\mathbf{q}} - L(\mathbf{q}, \dot{\mathbf{q}})$ . We can pay heed to the momenta which define for every  $\mathbf{q}$  a continuously differentiable bijection, i.e.  $\dot{\mathbf{q}} \leftrightarrow \mathbf{p}$ . This map is called the Legendre Transform, which we achieve since the linear momentum in classical mechanics is defined as  $\mathbf{p} = M(\mathbf{q}) \dot{\mathbf{q}}$ , so the existence of the Legendre transform is established. By replacing the variable  $\dot{\mathbf{q}} = M^{-1}(\mathbf{q}) \mathbf{p}$  in the definition of  $H$  we obtain

$$\begin{aligned} H &= \mathbf{p}^\top \dot{\mathbf{q}} - \left( \frac{1}{2} \dot{\mathbf{q}}^\top M(\mathbf{q}) \dot{\mathbf{q}} - V(\mathbf{q}) \right), \\ &= \frac{1}{2} \mathbf{p}^\top M^{-1}(\mathbf{q}) \mathbf{p} + V(\mathbf{q}). \end{aligned} \quad (2.31)$$

If in addition we consider an input matrix of forces  $G(\mathbf{q}) \mathbf{u}$ , i.e., the control forces, where  $\mathbf{u} \in \mathbb{R}^{n_u}$ , and  $G : \mathbb{R}^{n_q} \rightarrow \mathbb{R}^{n_q \times n_u}$ , then we can rewrite the Lagrange equations as  $\frac{d}{dt} \left( \frac{\partial L}{\partial \dot{q}_k} \right) - \frac{\partial L}{\partial q_k} = G(\mathbf{q}) \mathbf{u}$ , and we can present the pH structure by means of the canonical equations, thus

$$\begin{aligned} \begin{bmatrix} \dot{\mathbf{q}} \\ \dot{\mathbf{p}} \end{bmatrix} &= \begin{bmatrix} 0 & I \\ -I & 0 \end{bmatrix} \begin{bmatrix} \left( \frac{\partial H}{\partial \mathbf{q}} \right)^\top \\ \left( \frac{\partial H}{\partial \mathbf{p}} \right)^\top \end{bmatrix} + \begin{bmatrix} 0 \\ G(\mathbf{q}) \end{bmatrix} \mathbf{u}, \\ H(\mathbf{q}, \mathbf{p}) &= \frac{1}{2} \mathbf{p}^\top M^{-1}(\mathbf{q}) \mathbf{p} + V(\mathbf{q}). \end{aligned} \quad (2.32) \quad \text{(Hamiltonian)}$$

Equation (2.32) is well known as the (explicit) pH representation of a mechanical system. Similarly, we can consider the constraint equations  $\mathbf{g}(\mathbf{q}) = 0$ , with the arbitrary

functions  $\lambda$ , to find the implicit pH structure of a mechanical system<sup>5</sup>, that is

$$\begin{bmatrix} \dot{\mathbf{q}} \\ \dot{\mathbf{p}} \end{bmatrix} = \begin{bmatrix} 0 & I_{n_q} \\ -I_{n_q} & 0 \end{bmatrix} \begin{bmatrix} \left(\frac{\partial H}{\partial \mathbf{q}}\right)^\top \\ \left(\frac{\partial H}{\partial \mathbf{p}}\right)^\top \end{bmatrix} + \begin{bmatrix} 0 \\ b(\mathbf{q}) \end{bmatrix} \lambda + \begin{bmatrix} 0 \\ G(\mathbf{q}) \end{bmatrix} \mathbf{u}, \quad (2.33)$$

$$0 = b^\top(\mathbf{q}) \frac{\partial H}{\partial \mathbf{p}}, \quad (2.34)$$

$$H(\mathbf{q}, \mathbf{p}) = \frac{1}{2} \mathbf{p}^\top M^{-1}(\mathbf{p}) \mathbf{q} + V(\mathbf{q}), \quad (\text{Hamiltonian})$$

where  $b(\mathbf{q}) = (\partial \mathbf{g}(\mathbf{q}) / \partial \mathbf{q})^\top$  and Equation (2.34) is the time derivative of  $\mathbf{g}(\mathbf{q}) = 0$ , that is

$$\begin{aligned} 0 &= \left( \frac{\partial \mathbf{g}(\mathbf{q})}{\partial \mathbf{q}} \right) \frac{d\mathbf{q}}{dt} = b(\mathbf{q})^\top \dot{\mathbf{q}} \\ &= b(\mathbf{q})^\top \left( \frac{\partial H}{\partial \mathbf{p}} \right)^\top. \end{aligned}$$

#### 2.2.4 Underactuated Mechanical Systems

We can identify a fully actuated mechanical system if the input matrix  $G(\mathbf{q})$  is invertible, i.e.,  $\text{rank } G(\mathbf{q}) = n_u = n_q$ , and an UMS if  $\text{rank } G(\mathbf{q}) = n_u < n_q$ , in other words, a system that has fewer independent inputs than number of degrees of freedom. To check if an implicit system is underactuated we can follow [39] and define  $S = \begin{bmatrix} G(\mathbf{q}) & b(\mathbf{q}) \end{bmatrix}$ . Then we say the system is an UMS if  $\text{rank } S < n_q$ .

#### 2.2.5 Interconnection and Damping Assignment - PBC

The IDA-PBC was introduced in [40, 41]. The general idea is to find a passivity-based control law  $u$  on a system with pH structure as in Equation (2.29), such that the closed-loop has a desired or target pH structure and the equilibrium is asymptotically stable. To achieve the desired equilibrium  $(\mathbf{q}^*, 0)$  we need to shape the potential energy. For the case of UMS, shaping the potential may not be sufficient, thus, requiring to modify the kinetic energy, which implies solving a PDE [39]. This thesis focuses on the application of IDA-PBC to UMS. We consider the following desired closed-loop pH system

$$\sum^* : \quad \dot{x} = (J^*(x) - R^*(x)) \left( \frac{\partial H^*}{\partial x} \right)^\top, \quad (2.35)$$

---

<sup>5</sup>Note that we are using the same symbols for explicit and implicit structure. However, for the same physical system, the inertia matrix, the input matrix, the dissipation and the potential energy could change depending on the representation.

with  $(R^*(x))^\top = R^*(x) \geq 0$ ,  $(J^*(x))^\top = -J^*(x)$  and equilibrium point in  $\mathbf{x} = \mathbf{x}^*$ . Equating both systems, i.e.,  $\Sigma = \Sigma^*$ , gives place to the matching

$$G_u(\mathbf{x})\mathbf{u} = (J^*(\mathbf{x}) - R^*(\mathbf{x})) \left( \frac{\partial H^*}{\partial \mathbf{x}} \right)^\top - (J(\mathbf{x}) - R(\mathbf{x})) \left( \frac{\partial H}{\partial \mathbf{x}} \right)^\top. \quad (2.36)$$

To ensure (asymptotic) stability in the desired equilibrium  $\mathbf{x}^*$ , we apply Lyapunov's direct method. Thus, the following definiteness constraints must be satisfied

1.  $R^*$  is positive (semi-) definite, and
2. The desired Hamiltonian function  $H^*$  has a strict minimum at  $\mathbf{x} = \mathbf{x}^*$ .

**Lemma 2.** Let  $G_u$  be a matrix-valued map  $G_u : \mathcal{X} \rightarrow \mathbb{R}^{n_x \times n_u}$  with  $\text{rank}(G_u) = n_u < n_x$ . Define  $G_u^\perp \in \mathbb{R}^{(n_x - n_u) \times n_x}$  as the full rank left annihilator of  $G_u$ , i.e.,  $G_u^\perp G_u = 0$ . For any  $f \in \mathbb{R}^{n_x}$ ,  $\mathbf{u} \in \mathcal{U} \subseteq \mathbb{R}^{n_u}$

$$f(\mathbf{x}) + G_u(\mathbf{x})\mathbf{u} = 0 \Leftrightarrow \begin{cases} 0 &= G_u^\perp f(\mathbf{x}), \\ \mathbf{u} &= -(G_u^\top G_u)^{-1} G_u^\top f(\mathbf{x}). \end{cases} \quad (2.37)$$

*Proof.* The proof is completed using the annihilating property of  $G_u^\perp$  and noting that the square matrix  $G_u^\top G_u$  is invertible, see [30].  $\square$

**Remark.** As we seek for the control law  $u$  we need to perform the Moore-Penrose to Equation (2.36), i.e. first multiply both sides by  $G_u^\top$ , then by  $(G_u^\top G_u)^{-1}$ .

According to Lemma 2 we can choose a control law  $u$ , as presented in the following equation

$$\mathbf{u} = (G_u^\top G_u)^{-1} G_u^\top \left( (J^*(\mathbf{x}) - R^*(\mathbf{x})) \left( \frac{\partial H^*}{\partial \mathbf{x}} \right)^\top - (J(\mathbf{x}) - R(\mathbf{x})) \left( \frac{\partial H}{\partial \mathbf{x}} \right)^\top \right), \quad (2.38a)$$

$$0 = G_u^\perp \left( (J^*(\mathbf{x}) - R^*(\mathbf{x})) \left( \frac{\partial H^*}{\partial \mathbf{x}} \right)^\top - (J(\mathbf{x}) - R(\mathbf{x})) \left( \frac{\partial H}{\partial \mathbf{x}} \right)^\top \right). \quad (2.38b)$$

Therefore the matching problem is solved if and only if the matching condition Equation (2.38b) is satisfied. For the case of UMS we need to define some restrictions on the design of  $J^*$ ,  $R^*$  and/or on the closed loop Hamiltonian energy function  $H^*$ . Solving the matching condition is unduly a key step of this technique and it can be challenging to solve.

There are mainly three ways to proceed for the solution of the matching condition (2.38b). The most common approach is *Non-Parameterized IDA*, here the idea is to fix the

desired interconnection  $J^*(\mathbf{x})$  and dissipation matrices  $R^*(\mathbf{x})$ , hence its name. Additionally,  $G_u^\perp$  is fixed and  $H^*(\mathbf{x})$  is obtained from a set of *partial differential equations* PDEs given by Equation (2.38b). The energy function  $H^*(\mathbf{x})$  is chosen such that it has a strict minimum at the desired equilibrium  $\mathbf{x} = \mathbf{x}^*$ .

The *algebraic* IDA approach fixes the energy function, then Equation (2.38b) becomes an algebraic equation in  $J^*(\mathbf{x})$ ,  $R^*(\mathbf{x})$  and  $G_u^\perp$ .

The third approach is known as *Parameterized* IDA. Here, the structure of the desired energy function is restricted to a certain class. This restriction is motivated for some physical system, for instance, mechanical systems where the structure of the energy function is the sum of the kinetic and the potential energy, which are  $T$  and  $V$  respectively. This choice results in a different (and simpler) set of PDEs, however it also imposes some constraints in  $J^*(\mathbf{x})$  and  $R^*(\mathbf{x})$ .

This thesis centers on the application of the parameterized IDA to UMS. Therefore, we present the main considerations in order to determine a suitable control law  $\mathbf{u}_{ida}$ . Consider a pH structure of a mechanical system such as in Equation (2.32), where  $\mathbf{x} = [\mathbf{q}^\top \mathbf{p}^\top]^\top$ ,  $G_u = [0 \ G^\top]^\top$  and with passive output  $\mathbf{y} = G_u^\top (\partial H / \partial \mathbf{x})^\top$ .

**Definition 5 (Admissible equilibrium [30]).** *An equilibrium  $(\mathbf{q}^*, 0)$  (or simply  $\mathbf{q}^*$ ) of a mechanical system is called admissible if the following equality is satisfied*

$$G^\perp \left. \frac{\partial V(\mathbf{q})}{\partial \mathbf{q}} \right|_{\mathbf{q}^*} = 0 \quad (2.39)$$

We assign to the closed-loop a pH structure in accordance with mechanical systems, that is

$$\begin{aligned} \begin{bmatrix} \dot{\mathbf{q}} \\ \dot{\mathbf{p}} \end{bmatrix} &= \begin{bmatrix} 0 & J_1 \\ -J_1^\top & J_2 - R_2 \end{bmatrix} \begin{bmatrix} (\frac{\partial H^*}{\partial \mathbf{q}})^\top \\ (\frac{\partial H^*}{\partial \mathbf{p}})^\top \end{bmatrix}, \\ H^*(\mathbf{q}, \mathbf{p}) &= \frac{1}{2} \mathbf{p}^\top M^*(\mathbf{q})^{-1} \mathbf{p} + V^*(\mathbf{q}), \end{aligned} \quad (\text{Desired Energy Function}) \quad (2.40)$$

where  $M^* = M^*(\mathbf{q})$  is the desired symmetric and positive definite mass matrix,  $J_2$  is a skew symmetric matrix,  $R^* = \begin{bmatrix} 0 & 0 \\ 0 & R_2 \end{bmatrix}$  is a symmetric matrix. In this particular case the matching condition (2.36) becomes

$$\begin{bmatrix} 0 \\ G(\mathbf{q}) \end{bmatrix} \mathbf{u}_{ida} = \begin{bmatrix} 0 & J_1 \\ -J_1^\top & J_2 - R_2 \end{bmatrix} \begin{bmatrix} (\frac{\partial H^*}{\partial \mathbf{q}})^\top \\ (\frac{\partial H^*}{\partial \mathbf{p}})^\top \end{bmatrix} - \begin{bmatrix} 0 & I \\ -I & 0 \end{bmatrix} \begin{bmatrix} (\frac{\partial H}{\partial \mathbf{q}})^\top \\ (\frac{\partial H}{\partial \mathbf{p}})^\top \end{bmatrix}. \quad (2.41)$$

Due to the linear momenta  $\dot{\mathbf{q}} = M^{-1} \mathbf{p}$  which preserve in the closed loop, we have the relationship  $J_1 = M^{-1} M^*$ . Based on the result of Lemma 2, the control law that

satisfies (2.41) is

$$\mathbf{u}_{ida} = (G^\top G)^{-1} G^\top \left( \left( \frac{\partial H}{\partial \mathbf{q}} \right)^\top - J_1^\top \left( \frac{\partial H^*}{\partial \mathbf{q}} \right)^\top + [J_2 - R_2] \left( \frac{\partial H^*}{\partial \mathbf{p}} \right)^\top \right) \quad (2.42)$$

if and only if the PDE

$$G^\perp \left\{ \left( \frac{\partial H}{\partial \mathbf{q}} \right)^\top - J_1^\top \left( \frac{\partial H^*}{\partial \mathbf{q}} \right)^\top + [J_2 - R_2] \left( \frac{\partial H^*}{\partial \mathbf{p}} \right)^\top \right\} = 0 \quad (2.43)$$

is satisfied. Assuming  $R_2 = R_2(\mathbf{q})$ , and  $J_2 = J_{20}(\mathbf{q}) + J_{21}(\mathbf{q}, \mathbf{p})$ , with  $J_{21}$  linear in  $\mathbf{p}$ , the matching condition Equation (2.43) can be naturally split according to the dependency on  $\mathbf{p}$ , i.e. the terms quadratic and independent from  $\mathbf{p}$  correspond to the kinetic and potential energies, respectively [42]. Meanwhile the terms linear in  $\mathbf{p}$  correspond to the dissipation. Thus, (2.43) can be rewritten as

$$G^\perp \left( \left( \frac{\partial \mathbf{p}^\top M^{-1} \mathbf{p}}{\partial \mathbf{q}} \right)^\top - J_1^\top \left( \frac{\partial \mathbf{p}^\top M^*(\mathbf{q})^{-1} \mathbf{p}}{\partial \mathbf{q}} \right)^\top + 2 J_{21} M^*(\mathbf{q})^{-1} \mathbf{p} \right) = 0, \quad (2.44a)$$

$$G^\perp \left( \left( \frac{\partial V(\mathbf{q})}{\partial \mathbf{q}} \right)^\top - J_1^\top \left( \frac{\partial V^*(\mathbf{q})}{\partial \mathbf{q}} \right)^\top \right) = 0, \quad (2.44b)$$

$$G^\perp \left( [J_{20} - R_2] M^*(\mathbf{q})^{-1} \mathbf{p} \right) = 0. \quad (2.44c)$$

Equation (2.44a) is a non-homogeneous, first order quasilinear PDE that has to be solved to determine the unknown elements of the desired mass matrix  $M^*(\mathbf{q})$ . For a given desired mass matrix, Equation (2.44b) becomes a linear PDE for the unknown function  $V^*(\mathbf{q})$ , and the third equation, Equation (2.44c) is a simple algebraic equation, which can be solved by choosing

$$J_{20} - R_2 = G(K_j - K_v)G^\top \quad (2.45)$$

with free parameters  $K_j$  and  $K_v$  where  $K_j = -K_j^\top \in \mathbb{R}^{n_u \times n_u}$ , and  $K_v = K_v^\top > 0$ . Is important to note that  $R_2 := G K_v G^\top$ , this choice is later explained, but the main reason is due to the relationship between the time derivative of the desired energy function

$$\frac{dH^*(\mathbf{q}, \mathbf{p})}{dt} = \left( \frac{\partial H^*}{\partial \mathbf{q}} \right) \dot{\mathbf{q}} + \left( \frac{\partial H^*}{\partial \mathbf{p}} \right) \dot{\mathbf{p}} \quad (2.46)$$

and the so-called passive output of the closed-loop, which is defined by

$$\mathbf{y}^* = G^\top \left( \frac{\partial H^*}{\partial \mathbf{p}} \right)^\top. \quad (2.47)$$



**Corollary 1 (Stability of the closed-loop system [30]).** *Consider the system (2.32) with desired closed loop system (2.40),  $R_2 := G K_v G^\top$ , and control law (2.42). If*

$$\mathbf{q}^* = \arg \min V^*, \quad M^*(\mathbf{q}) = M^*(\mathbf{q})^\top > 0 \quad \text{and} \quad R_2 \geq 0 \quad (2.48)$$

*in a neighborhood of  $\mathbf{q}^*$ , then the equilibrium  $\mathbf{q}^*$  is (locally) stable with Lyapunov function  $H^*$ . Asymptotic stability follows if the closed loop system is zero-state detectable from the output  $y^*$ .*

*Proof.* Replacing  $\dot{\mathbf{q}}$  and  $\dot{\mathbf{p}}$  from the closed loop system (2.40) in (2.46) yields

$$\frac{dH^*(\mathbf{q}, \mathbf{p})}{dt} = \left( \frac{\partial H^*}{\partial \mathbf{p}} \right) (J_2 - R_2) \left( \frac{\partial H^*}{\partial \mathbf{p}} \right)^\top. \quad (2.49)$$

with  $J_2 = -J_2^\top$  and  $R_2 := G K_v G^\top$ . Then, replacing the passive output in Equation (2.49) results in

$$\frac{dH^*(\mathbf{q}, \mathbf{p})}{dt} = -(\mathbf{y}^*)^\top K_v \mathbf{y}^* \leq -\lambda_{\min} \{K_v\} \|\mathbf{y}^*\|_2^2 \leq 0 \quad (2.50)$$

Asymptotic stability, under the zero-state detectability condition, is established invoking Barbashin-Krasovskii, see [36]. □

---

## Chapter 3

# Implicit IDA-PBC for UMS

---

This chapter addresses the systematic design of passivity-based controllers for implicit port Hamiltonian structures of underactuated mechanical systems (UMS)s. Therefore, the energy shaping method will be introduced to implicit pH structures. The mathematical concepts here presented are borrowed from [4, 37].

### 3.1 Problem formulation

In Section 2.2.5 the IDA-PBC methodology was presented for UMSs, where we found a state feedback (2.42) through the solution of the matching problem (2.41). We also observed that it is possible to represent a mechanical system in implicit pH structure. In view of this, three questions naturally arise:

1. Is it possible to find a suitable control law for UMS in implicit pH representation?
2. If we shape the energy of a mechanical system with constraints, is it possible to find a general structure for the desired mass matrix?
3. Can we find an output-feedback law?

These three questions are answered by Cieza and Reger in [4]. The purpose of this chapter is to present the general idea of the Implicit IDA-PBC approach and later in Chapter 4, implement it on a physical system, namely, the portal crane.

### 3.2 Implicit IDA-PBC for holonomic systems

As presented in Section 2.2.3, let us briefly recapitulate the implicit<sup>6</sup> representation of a mechanical system given by

$$\begin{bmatrix} \dot{\mathbf{r}} \\ \dot{\boldsymbol{\rho}} \end{bmatrix} = \begin{bmatrix} 0 & I_{n_q} \\ -I_{n_q} & 0 \end{bmatrix} \begin{bmatrix} (\frac{\partial \mathcal{H}}{\partial \mathbf{r}})^\top \\ (\frac{\partial \mathcal{H}}{\partial \boldsymbol{\rho}})^\top \end{bmatrix} + \begin{bmatrix} 0 \\ \mathbf{b}(\mathbf{r}) \end{bmatrix} \boldsymbol{\lambda} + \begin{bmatrix} 0 \\ \mathcal{G}(\mathbf{r}) \end{bmatrix} \mathbf{u}, \quad (3.1a)$$

$$\mathbf{b}^\top(\mathbf{r}) \frac{\partial \mathcal{H}}{\partial \boldsymbol{\rho}} = 0, \quad (3.1b)$$

$$\mathcal{H}(\mathbf{r}, \boldsymbol{\rho}) = \frac{1}{2} \boldsymbol{\rho}^\top \mathcal{M}(\mathbf{r})^{-1} \boldsymbol{\rho} + \mathcal{V}(\mathbf{r}), \quad (\text{Hamiltonian})$$

where  $\mathbf{r} \in \mathbb{R}^{n_r}$  and  $\boldsymbol{\rho} \in \mathbb{R}^{n_r}$  are implicit generalized coordinates (position and its canonical momenta, respectively),  $\mathbf{u} \in \mathbb{R}^{n_u}$  is the input and  $\mathcal{G} : \mathbb{R}^{n_r} \rightarrow \mathbb{R}^{n_r \times n_u}$  is the implicit full rank input matrix. The  $n_\lambda$  holonomic constraints  $\mathbf{g}(\mathbf{r}) = 0$  and the arbitrary functions (or implicit variables)  $\boldsymbol{\lambda} \in \mathbb{R}^{n_\lambda}$  are related by the constraints forces  $\mathbf{b}(\mathbf{r}) \boldsymbol{\lambda}$  where  $(\partial \mathbf{g}(\mathbf{r}) / \partial \mathbf{r})^\top = \mathbf{b}(\mathbf{r}) : \mathbb{R}^{n_r} \rightarrow \mathbb{R}^{n_r \times n_\lambda}$ . The velocity in implicit coordinates is  $\dot{\mathbf{r}} \equiv (\partial \mathcal{H} / \partial \boldsymbol{\rho})^\top = \mathcal{M}(\mathbf{r})^{-1} \boldsymbol{\rho}$ , where  $\mathcal{M}(\mathbf{r}) : \mathbb{R}^{n_r} \rightarrow \mathbb{R}^{n_r \times n_r}$  is the symmetric positive definite mass matrix and the Hamiltonian  $\mathcal{H} : \mathbb{R}^{n_r} \times \mathbb{R}^{n_r} \rightarrow \mathbb{R}$  represents the total energy function. We say that (3.1) is an UMS if  $\text{rank } S < n_r$ , where  $S = [\mathcal{G}(\mathbf{r}) \ \mathbf{b}(\mathbf{r})]$ .

**Proposition 1** (Well-posedness [4]). *Consider the holonomic system (3.1). Then for all  $\mathbf{r} \in \mathcal{X} = \{\mathbf{r} \in \mathbb{R}^{n_r} \mid \text{rank } \Delta = n_\lambda\}$ ,  $\Delta := \mathbf{b}^\top(\mathbf{r}) \mathcal{M}(\mathbf{r})^{-1} \mathbf{b}(\mathbf{r})$ , the constrained state-space set*

$$\mathcal{X}_c = \{(\mathbf{r}, \boldsymbol{\rho}) \in \mathcal{X} \times \mathbb{R}^{n_r} \mid \mathbf{b}^\top(\mathbf{r}) (\frac{\partial \mathcal{H}}{\partial \boldsymbol{\rho}})^\top = 0, \quad g_k(\mathbf{r}) = 0\}$$

is a regular manifold embedded in  $\mathbb{R}^{n_r} \times \mathbb{R}^{n_r}$ , and (3.1) described by Differential-Algebraic Equations (DAEs) has differential index 1 with unique solution for  $\boldsymbol{\lambda}$ . Here,

$$g_k(\mathbf{r}) = \int_0^{\mathbf{r}} b_k^\top(s) ds + c_i \equiv 0, \quad (3.2)$$

is the general expression for the integrated constrains, i.e.,  $\mathbf{b}(\mathbf{r}) = (\partial \mathbf{g}(\mathbf{r}) / \partial \mathbf{r})^\top$ ,  $b_k$  is the  $k$ th column vector of  $\mathbf{b}(\mathbf{r})$ ,  $c_i$  is a constant and  $\partial \mathcal{H} / \partial \boldsymbol{\rho} \mathbf{b}(\mathbf{r})$  differentiable.

<sup>6</sup>We write now  $\mathbf{r}$  instead of  $\mathbf{q}$ ,  $\boldsymbol{\rho}$  instead of  $\mathbf{p}$ ,  $\mathcal{H}$  instead of  $H$ ,  $\mathcal{V}$  instead of  $V$ ,  $\mathcal{M}$  instead of  $M$  and  $\mathcal{G}$  instead of  $G$  with the purpose to be aware that we are dealing with the implicit pH representation.

Similar to the explicit IDA-PBC, we define the desired closed-loop pH system

$$\begin{bmatrix} \dot{\mathbf{r}} \\ \dot{\boldsymbol{\rho}} \end{bmatrix} = \begin{bmatrix} 0 & \mathcal{J}(\mathbf{r}) \\ -\mathcal{J}^\top(\mathbf{r}) & -\mathcal{W}(\mathbf{r}, \boldsymbol{\rho}) \end{bmatrix} \begin{bmatrix} \left(\frac{\partial \mathcal{H}_d}{\partial \mathbf{r}}\right)^\top \\ \left(\frac{\partial \mathcal{H}_d}{\partial \boldsymbol{\rho}}\right)^\top \end{bmatrix} + \begin{bmatrix} 0 \\ b_d(\mathbf{r}) \end{bmatrix} \boldsymbol{\lambda}_d, \quad (3.3a)$$

$$0 = b_d^\top(\mathbf{r}) \frac{\partial \mathcal{H}_d}{\partial \boldsymbol{\rho}}, \quad (3.3b)$$

$$\mathcal{H}_d(\mathbf{r}, \boldsymbol{\rho}) = \frac{1}{2} \boldsymbol{\rho}^\top \mathcal{M}_d(\mathbf{r})^{-1} \boldsymbol{\rho} + \mathcal{V}_d(\mathbf{r}), \quad (\text{Desired Hamiltonian})$$

where the desired dynamics are well defined for all

$$\mathbf{r} \in \mathcal{X}_d = \{\mathbf{r} \in \mathbb{R}^{n_r} \mid \text{rank } \Delta_d = n_\lambda\}, \quad \Delta_d := b_d^\top(\mathbf{r}) \mathcal{M}_d(\mathbf{r})^{-1} b_d(\mathbf{r}).$$

The desired Hamiltonian  $\mathcal{H}_d = \mathcal{H}_d(\mathbf{r}, \boldsymbol{\rho})$  is the new shaped energy function,  $\boldsymbol{\lambda}_d \in \mathbb{R}^{n_\lambda}$  are the new implicit variables in closed-loop,  $\mathcal{M}_d = \mathcal{M}_d(\mathbf{r})$  is the nonsingular symmetric desired mass matrix,  $\mathcal{J}: \mathcal{X}_d \rightarrow \mathbb{R}^{n_r \times n_r}$  is nonsingular, and  $\mathcal{W} = \mathcal{W}(\mathbf{r}, \boldsymbol{\rho}): \mathcal{X}_d \times \mathbb{R}^{n_r} \rightarrow \mathbb{R}^{n_r \times n_r}$ .

As before we are dealing with mechanical systems, thus, the momenta are preserved in the closed-loop, i.e.  $(\partial \mathcal{H}_d / \partial \boldsymbol{\rho})^\top = \mathcal{M}_d^{-1} \boldsymbol{\rho} \Rightarrow \mathcal{J} = \mathcal{M}^{-1} \mathcal{M}_d$ . Besides, the physical property (3.1b) is equivalently represented as (3.3b), then equating both results in  $b_d = \mathcal{J}^\top b(\mathbf{r})$ . Next, we equate (3.1a) and (3.3a), resulting in

$$\underbrace{\begin{bmatrix} \mathcal{G}(\mathbf{r}) & b(\mathbf{r}) \end{bmatrix}}_{=: S} \begin{bmatrix} \mathbf{u} \\ \boldsymbol{\lambda} \end{bmatrix} = \left(\frac{\partial \mathcal{H}}{\partial \mathbf{r}}\right)^\top - \mathcal{J}^\top \left(\frac{\partial \mathcal{H}_d}{\partial \mathbf{r}}\right)^\top - \mathcal{W} \left(\frac{\partial \mathcal{H}_d}{\partial \boldsymbol{\rho}}\right)^\top + \mathcal{J}^\top b_d(\mathbf{r}) \boldsymbol{\lambda}_d. \quad (3.4)$$

Then, similar to Lemma 2, we have

$$\begin{bmatrix} \mathbf{u} \\ \boldsymbol{\lambda} \end{bmatrix} = (S^\top S)^{-1} S^\top \left( \left(\frac{\partial \mathcal{H}}{\partial \mathbf{r}}\right)^\top - \mathcal{J}^\top \left(\frac{\partial \mathcal{H}_d}{\partial \mathbf{r}}\right)^\top - \mathcal{W} \left(\frac{\partial \mathcal{H}_d}{\partial \boldsymbol{\rho}}\right)^\top + \mathcal{J}^\top b_d(\mathbf{r}) \boldsymbol{\lambda}_d \right) \quad (3.5a)$$

$$0 = S^\perp \left( \left(\frac{\partial \mathcal{H}}{\partial \mathbf{r}}\right)^\top - \mathcal{J}^\top \left(\frac{\partial \mathcal{H}_d}{\partial \mathbf{r}}\right)^\top - \mathcal{W} \left(\frac{\partial \mathcal{H}_d}{\partial \boldsymbol{\rho}}\right)^\top + \mathcal{J}^\top b_d(\mathbf{r}) \boldsymbol{\lambda}_d \right). \quad (3.5b)$$

Where  $S^\perp$  is the full rank left annihilator of  $S$ . The implicit matching problem is solved through the following propositions

**Proposition 2** (Implicit Matching [43]). *The implicit feedback  $u = u_I$ ,*

$$u_I = S^\dagger \left( \left(\frac{\partial \mathcal{H}}{\partial \mathbf{r}}\right)^\top - \mathcal{J}^\top \left(\frac{\partial \mathcal{H}_d}{\partial \mathbf{r}}\right)^\top - \mathcal{W} \left(\frac{\partial \mathcal{H}_d}{\partial \boldsymbol{\rho}}\right)^\top + \mathcal{J}^\top b(\mathbf{r}) \boldsymbol{\lambda}_d \right) \quad (3.6)$$

transforms the system (3.1) into (3.3) for any trajectory of  $\mathbf{r}$  that remains in  $\mathcal{X} \cap \mathcal{X}_d$ , whenever the implicit matching conditions

$$S^\perp \left( \left( \frac{\partial \mathcal{M}(\mathbf{r})^{-1} \rho}{\partial \mathbf{r}} \right)^\top - \mathcal{J}^\top \left( \frac{\partial \mathcal{M}_d(\mathbf{r})^{-1} \rho}{\partial \mathbf{r}} \right)^\top - \mathcal{W}_1 \mathcal{M}_d(\mathbf{r})^{-1} \right) \rho = 0, \quad (3.7a)$$

$$S^\perp \left( \left( \frac{\partial \mathcal{V}(\mathbf{r})}{\partial \mathbf{r}} \right)^\top - \mathcal{J}^\top \left( \frac{\partial \mathcal{V}_d(\mathbf{r})}{\partial \mathbf{r}} \right)^\top \right) = 0, \quad (3.7b)$$

$$S^\perp \left( \mathcal{J}^\top b(\mathbf{r}) \right) = 0, \quad (3.7c)$$

are satisfied with  $\mathcal{J} = \mathcal{M}^{-1} \mathcal{M}_d$ ,  $b_d(\mathbf{r}) = \mathcal{J}^\top b(\mathbf{r})$ ,  $S^\dagger = [I_{n_u} \ 0](S^\top S)^{-1} S^\top$ ,

$$\mathcal{W}(\mathbf{r}, \boldsymbol{\rho}) = \frac{1}{2} \mathcal{W}_1(\mathbf{r}, \boldsymbol{\rho}) + S K_u(\mathbf{r}) S^\top, \quad (3.8)$$

$K_u = K_u(\mathbf{r}) \in \mathbb{R}^{(n_u+n_\lambda) \times (n_u+n_\lambda)}$  and  $\mathcal{W}_1 = \mathcal{W}_1(\mathbf{r}, \boldsymbol{\rho}) \in \mathbb{R}^{n_r \times n_r}$ .

**Remark.** We can compute  $\boldsymbol{\lambda}$  or  $\boldsymbol{\lambda}_d$  through, the hidden constraints, i.e., the time derivative of (3.1b) or (3.3b).

$$\begin{aligned} \frac{d \left( b^\top \mathcal{M}^{-1} \rho \right)}{dt} &= \frac{\partial \left( b^\top \mathcal{M}^{-1} \rho \right)}{\partial \mathbf{r}} \dot{\mathbf{r}} + \frac{\partial \left( b^\top \mathcal{M}^{-1} \rho \right)}{\partial \boldsymbol{\rho}} \dot{\boldsymbol{\rho}} = 0 \\ \Rightarrow \boldsymbol{\lambda} &= \Delta^{-1} \left[ \left( -\frac{\partial \left( b^\top \mathcal{M}^{-1} \rho \right)}{\partial \mathbf{r}} \dot{\mathbf{r}} \right) - \left( b^\top \mathcal{M}^{-1} \left( \mathcal{G}(\mathbf{r}) u_I - \left( \frac{\partial \mathcal{H}}{\partial \mathbf{r}} \right)^\top \right) \right) \right] \end{aligned} \quad (3.9)$$

**Proposition 3** (Implicit stability [43]). Assume that the conditions of Proposition 2 are satisfied for an holonomic system, and define the new domain

$$\mathcal{X}_I = (\{\mathbf{r} \in \mathcal{X}_d \mid b^\perp \mathcal{M} \mathcal{M}_d^{-1} \mathcal{M} (b^\perp)^\top \succ 0\} \times \mathbb{R}^{n_r}) \cap \mathcal{X}_c.$$

The closed-loop system (3.3) has a stable equilibrium in

$$x^* = (\mathbf{r}^*, 0) \in \mathcal{X}_a = \left\{ x \in \mathcal{X}_I \mid S^\perp \left( \frac{\partial \mathcal{V}(\mathbf{r})}{\partial \mathbf{r}} \right)^\top = 0 \right\}$$

for any  $K_u(\mathbf{r}) + K_u^\top(\mathbf{r}) \succeq 0$  if

$$r^* = \arg \min_{r \in \mathcal{X}_I} \mathcal{V}_d \quad (3.10)$$

is an isolated minimum and

$$0 = \rho^\top \mathcal{M}_d^{-1} \mathcal{W}_1 \mathcal{M}_d^{-1} \rho \Big|_{\mathcal{X}_I}. \quad (3.11)$$

Furthermore, if

$$y_I = (K_u(\mathbf{r}) + K_u^\top(\mathbf{r}))^{\frac{1}{2}} \mathcal{M}_d^{-1} \rho \quad (3.12)$$

is a detectable output of (3.3),  $x^*$  is asymptotically stable.

*Proof.* The definition of  $\mathcal{X}_d$  assures well-defined dynamics of (3.3a) under (3.3b). The transformation of the implicit pH structure (3.1) to a closed-loop implicit structure (3.3) is possible by noting that the control law (3.6) and the implicit matching equations (3.7) are sufficient conditions for (3.5). Besides, such mechanical structure transformation implies  $\mathcal{J} = \mathcal{M}^{-1} \mathcal{M}_d$ ,  $b_d = \mathcal{J}^\top b$ . Since all constraints are integrable, define the Lagrangian function

$$\mathcal{L}_d(\mathbf{r}, \boldsymbol{\rho}, \boldsymbol{\nu}, \boldsymbol{\mu}) := \mathcal{H}_d + \boldsymbol{\nu}^\top b^\top \mathcal{M}^{-1} \boldsymbol{\rho} + \boldsymbol{\mu}^\top \mathbf{g} \quad (3.13)$$

with Lagrange multipliers  $\boldsymbol{\mu}$  and  $\boldsymbol{\nu}$  and constraints  $\mathbf{g}$ . Then, seeking for a minimum (or maximum) of  $\mathcal{H}_d|_{\mathcal{X}_c}$ , the following expression should be satisfied

$$\left( \frac{\partial \mathcal{L}_d(\mathbf{r}^*, \boldsymbol{\rho}^*, \boldsymbol{\nu}^*, \boldsymbol{\mu}^*)}{\partial \mathbf{x}} \right)^\top = 0, \quad (3.14)$$

with

$$\left( \frac{\partial \mathcal{L}_d(\mathbf{r}, \boldsymbol{\rho}, \boldsymbol{\nu}, \boldsymbol{\mu})}{\partial \mathbf{x}} \right)^\top = \begin{bmatrix} \left( \frac{\partial \mathcal{L}_d}{\partial \mathbf{r}} \right)^\top \\ \left( \frac{\partial \mathcal{L}_d}{\partial \boldsymbol{\rho}} \right)^\top \end{bmatrix} = \begin{bmatrix} \left( \frac{\partial \mathcal{V}_d}{\partial \mathbf{r}} \right)^\top + \left( \frac{\partial \boldsymbol{\rho}^\top \mathcal{M}^{-1} b \boldsymbol{\nu}}{\partial \mathbf{r}} \right)^\top + b \boldsymbol{\mu} \\ \mathcal{M}^{-1} b \boldsymbol{\nu} + \mathcal{M}_d^{-1} \boldsymbol{\rho} \end{bmatrix}. \quad (3.15)$$

Multiplying on the left by  $\begin{bmatrix} b & (b^\perp)^\top \end{bmatrix}^\top \mathcal{M}^{-1} \mathcal{M}_d$ , and taking advantage of the full rank condition of  $\Delta_d$ , Equation (3.14) is reduced to

$$\boldsymbol{\rho}^* = 0, \quad \boldsymbol{\nu}^* = 0, \quad \text{and,} \quad \left( \frac{\partial \mathcal{V}_d(\mathbf{r}^*)}{\partial \mathbf{r}} \right)^\top + \mathbf{b}(\mathbf{r}^*) \boldsymbol{\mu}^* = 0. \quad (3.16)$$

Replacing  $x^* = (\mathbf{r}^*, \boldsymbol{\rho}^*)$ , (3.14) and (3.7c) in (3.7b), yields

$$S^\perp(\mathbf{r}^*) \left( \frac{\partial \mathcal{V}(\mathbf{r}^*)}{\partial \mathbf{r}} \right)^\top = 0, \quad (3.17)$$

which represents the attainable set  $\mathcal{X}_d$ . We might now employ  $\mathbf{r}^* = \arg \min \mathcal{V}_d|_{\mathcal{X}_I}$  and Finsler's Lemma on  $\rho^\top \mathcal{M}_d^{-1}(\mathbf{r})\rho$  subject to (3.3b), obtaining

$$\mathcal{H}_d > 0 \quad \text{iff} \quad x \in \mathcal{X}_I \quad \text{and} \quad \mathcal{V}_d(\mathbf{r}^*) = 0. \quad (3.18)$$

Stability in  $x^*$  can be demonstrated if we use  $\mathcal{H}_d$  as Lyapunov Function for  $x \in \mathcal{X}_I$  with minimum at  $x^*$  and time derivative

$$\dot{\mathcal{H}}_d(\mathbf{r}, \rho) = -\rho^\top \mathcal{M}_d(\mathbf{r})^{-1} \mathcal{W} \mathcal{M}_d(\mathbf{r})^{-1} \rho \Big|_{\mathcal{X}_I} \leq 0. \quad (3.19)$$

Finally, applying Barbashin-Krasovskii-LaSalle's Theorem implies convergence of  $y_I$  to 0. Therefore, asymptotically stability in  $x^*$  is reached if  $y_I$  is a detectable output of (3.3).  $\square$

**Remark.**  $\mathcal{M}_d$  is a full rank matrix but not necessarily  $\mathcal{M}_d \succ 0$ . Also, it is important to notice that the matching condition (3.7c) introduces conservativeness and allows to reduce complexity solving (3.7a) and (3.7b) independently of  $\lambda_d$ , even though the latter is required for the controller (3.6).

### 3.2.1 Mechanical systems with constant mass matrix

One may claim that the implicit matching conditions are quite complicated to solve. However, the main advantage lies on systems that have a constant mass matrix. That means that the mass matrix modeled in the Euclidean space has no dependence on the generalized coordinates. However, in the explicit representation, it may indeed possess that dependence. The following proposition avoids solving the kinetic PDE (3.7a).

**Proposition 4** (Algebraic Implicit IDA-PBC [4]). *Consider an implicit pH system (3.1) with only holonomic constraints. Assume, additionally, that (3.1) is well-posed and possesses a constant mass matrix  $\mathcal{M}$ , a linear potential energy  $\mathcal{V}(\mathbf{r})$ , and polynomial  $\mathcal{G}(\mathbf{r})$  and  $\mathbf{g}(\mathbf{r})$ . The feedback (3.6) stabilizes the closed-loop (3.3) at the equilibrium  $\mathbf{x}^* = (\mathbf{r}^*, 0)$ , with  $K_u + K_u^\top \succeq 0$  if, there*

- (i) exist a constant vector  $\mu^* \in \mathbb{R}^{n_\lambda}$ ,
- (ii) exist a matrix  $A \in \mathbb{R}^{(n_r - n_\lambda) \times (n_r - n_\lambda)}$  with  $A = A^\top \succ 0$ ,
- (iii) exist a matrix  $C \in \mathbb{R}^{(n_r - n_\lambda) \times n_\lambda}$ ,
- (iv) exist a non-singular matrix  $D \in \mathbb{R}^{n_\lambda \times n_\lambda}$  with  $D = D^\top$ , and
- (v) exist a matrix  $\bar{S}(\mathbf{r}) \in \mathbb{R}^{(n_u + n_\lambda) \times n_\psi}$ , where  $n_\psi \leq n_u + n_\lambda$  and  $\bar{S}_i$  is the  $i$ th column of  $\bar{S}$

such that

$$S^\perp \left( \left( \frac{\partial \mathcal{V}}{\partial \mathbf{r}} \right)^\top + \mathcal{M} Z_c D b^{*\top} \mu^* \right) = 0, \quad (3.20a)$$

$$S^\perp \mathcal{M} \left( (b^{*\perp})^\top A b^{*\perp} + Z_c D Z_c^\top \right) b = 0, \quad (3.20b)$$

$$\frac{\partial(S \bar{S}_i)}{\partial \mathbf{r}} \mathcal{M}^{-1} \mathcal{M}_d - \mathcal{M}_d \mathcal{M}^{-1} \left( \frac{\partial(S \bar{S}_i)}{\partial \mathbf{r}} \right)^\top = 0, \quad (3.20c)$$

$$Z^\perp Z_a (Z^\perp)^\top \succ 0, \quad (3.20d)$$

where

$$\mathcal{M}_d := \mathcal{M} B^* \begin{bmatrix} A + CDC^\top & CD \\ DC^\top & D \end{bmatrix} B^{*\top} \mathcal{M}, \quad (3.21)$$

$$\mathcal{V}_d := \frac{1}{2} \psi^\top K_\psi \psi + \tilde{\mathbf{r}}^\top b^* \mu^*, \quad (3.22)$$

$B^{*\top} = \begin{bmatrix} b^* \\ b^{*\top} \end{bmatrix}$ ,  $\psi(r) = \int_{r^*}^r \bar{S}_i^\top(s) \mathcal{M}_d^{-1} \mathcal{M} ds$ ,  $\tilde{\mathbf{r}} := \mathbf{r}^* - \mathbf{r}$ ,  $b^* = b(\mathbf{r}^*)$ ,  $Z_c = (b^{*\perp})^\top C + b^*$ ,  $Z_a = A b^{*\perp} \partial b \mu^* / \partial \mathbf{r} |_{r=r^*} (b^{*\perp})^\top A$ ,  $Z = [I_{n_r - n_\lambda} \ -C] B^{*-1} \mathcal{M}^{-1} S(\mathbf{r}) \bar{S}(\mathbf{r}^*)$  has full rank,

$$\left[ (S^\perp)^\top \ \mathcal{M}_d^{-1} \right]^\top \mathcal{W}_1 = 0, \quad (3.23a)$$

$$K_\psi \succ -Z^\dagger \left( Z_a - Z_a (Z^\perp)^\top (Z^\perp Z_a (Z^\perp)^\top)^{-1} \right) Z^{\dagger\top}, \quad (3.23b)$$

$K_\psi \in \mathbb{R}^{n_\psi \times n_\psi}$  is symmetric, and  $Z^\dagger = (Z^\top Z)^{-1} Z^\top$ . Moreover if  $y_I$  is a detectable output, then (3.3) is asymptotically stable.

*Proof.* It begins by observing that  $\mathcal{V}_d$  exists due to the existence of  $\psi$  by the integrability condition (3.20c). Similar to the proof of Proposition 3 we need a Lagrange function  $\mathcal{L}_d$  as presented in (3.13), thus  $\mu^* \in \mathbb{R}^{n_\lambda}$ . Then, direct substitution of  $\mathcal{H}_d$  in (3.7) with (3.23a), results in (3.20a)–(3.20b) and fulfills (3.7a) and (3.11). The next step is to make  $x^*$  a strict (local) minimum of  $\mathcal{H}_d|_{\mathcal{X}_c}$ . The necessary and sufficient conditions (see [44]) for this are (3.14) and

$$y_\rho^\top \mathcal{M}_d^{-1} y_\rho > 0, \quad \forall y_\rho \quad \text{with} \quad y_\rho^\top M^{-1} b^* = 0, \quad \text{and},$$

$$y_r^\top \left( \frac{\partial^2 \mathcal{V}_d}{\partial \mathbf{r}^2} + \frac{\partial(b \mu^*)}{\partial \mathbf{r}} \right) \Big|_{r=r^*} y_r > 0, \quad \forall y_r \quad \text{with} \quad y_r^\top b^* = 0$$



Now, we can use Finsler's Lemma and replace  $\psi$ ,  $\mathcal{J}$  and  $\mathcal{M}_d$  in the above inequalities<sup>7</sup> which results in

$$b^\perp \mathcal{M} \mathcal{M}_d^{-1} \mathcal{M} (b^\perp)^\top \Big|_{\mathbf{r}=\mathbf{r}^*} = A^{-1}, \quad (3.24a)$$

$$Z K_\psi Z^\top + Z_a \succ 0. \quad (3.24b)$$

Inequality (3.24a) is equivalent to  $A \succ 0$ . We can obtain (3.20d) and (3.23b) if we multiply (3.24b) on both sides by adequate full rank matrices and use Schur's complement. Straightforward calculations in  $\mathbf{r}^*$  show that  $\Delta_d(\mathbf{r}^*) = (b^*)^\top b^* D (b^*)^\top b^*$  is full rank, which implies that  $x^*$  is a strict (local) minimum of  $\mathcal{H}_d|_{\mathcal{X}_I \subseteq \mathcal{X}_c}$ . Thus, the desired pH structure in closed-loop is (asymptotically) stable in a neighborhood of  $x^*$ .  $\square$

Figure 3.1 shows how to perform the algorithm<sup>8</sup>. The algorithm begins by selecting  $\mathbf{r}^*$  and adequate full rank left annihilators  $S^\perp$  and  $b^\perp$ . Afterwards, we find a numerical solution of  $C$  (if possible) and constraints inequalities in  $A$ ,  $D$  and  $\mu^*$  aided by the implicit matching conditions (3.20a) and (3.20b). In the next step, assisted by (3.20c), we select  $\bar{S}$ , calculate  $Z$  and then select its full rank left annihilator  $Z^\perp$ . Finally, use (3.20d), (3.23) and  $K_u + K_u^\top \succeq 0$  to choose  $A \succ 0$ ,  $W_1$ , non-singular  $D$ ,  $\mu^*$ ,  $K_\psi$  and  $K_u$ .

**Remark.** It is possible to consider  $K_\psi$  as a matrix function of  $\mathbf{r}$ , i.e.,  $K_\psi = K_\psi(\mathbf{r})$ . However,  $K_\psi(\mathbf{r}^*)$  has to fulfill Equation (3.23b). Although, taking this into practice may influence the region of attraction.

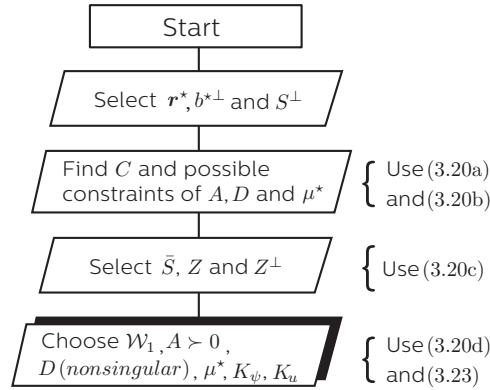


Figure 3.1. – Algorithm for the algebraic implicit IDA-PBC

<sup>7</sup>The inversion of  $\mathcal{M}_d$  can be reached if the Schur complement is performed.

<sup>8</sup>A requirement is to have the system in implicit pH structure. Thus, we can easily identify  $G$ ,  $b$  and  $S$ .

### 3.2.2 Position feedback

As we mentioned in Section 3.1 it is possible to produce a simple dynamic feedback that obviates the velocity measurement. In order to do this, we need some additional requirements.

**Proposition 5** (Output-feedback [4]). *Let the conditions of Proposition 4 be satisfied with  $S\bar{S} = \mathcal{G}$  and  $\mathcal{W}_1 = 0$  if, additionally,  $b^\perp \mathcal{J}^\top b = 0$ , the new control law*

$$u_N = S^\dagger \left( \left( \frac{\partial \mathcal{H}}{\partial \mathbf{r}} \right)^\top - \mathcal{J}^\top \left( \frac{\partial \mathcal{V}_d}{\partial \mathbf{r}} \right)^\top - \mathcal{G} \bar{K}_u (\xi + \bar{\psi}(\mathbf{r})) \right), \quad (3.25a)$$

$$\dot{\xi} = -\Lambda_\xi(\mathbf{r}) \bar{K}_u (\xi + \bar{\psi}(\mathbf{r})) \quad (3.25b)$$

with  $\bar{K}_u = \bar{K}_u^\top$ ,  $\Lambda_\xi + \Lambda_\xi^\top \succ 0$ ,  $\partial\psi/\partial\mathbf{r} = \mathcal{G}^\top \mathcal{M}_d^{-1} \mathcal{M}$ ,  $\xi \in \mathbb{R}^{n_u}$ ,  $\Lambda_\xi, \bar{K}_u \in \mathbb{R}^{n_u \times n_u}$ , and  $\mathcal{H}_d$  as in Prop. 4, stabilizes the system at  $x^*$ . Moreover, the closed-loop is asymptotically stable if the system (3.3a) is zero state detectable with respect to the output  $y_N = \mathcal{G}^\top \mathcal{M}_d^{-1} \rho$ .

*Proof.* Assume the conditions of Proposition (4) are met. Then, closing the loop of the implicit pH system (2.2.3) with  $u_N$ ,  $b^\perp \mathcal{J}^\top b = 0$  or its equivalent  $\mathcal{J}^\top b = bk$  (for some square matrix  $k$ ),  $S\bar{S} = \mathcal{G}$ , and  $\dot{\psi} = \mathcal{G}^\top \mathcal{M}_d^{-1} \rho$ , results in a ‘new’ structure for the implicit closed loop system, that is

$$\begin{bmatrix} \dot{\mathbf{r}} \\ \dot{\rho} \\ \dot{\tilde{\xi}} \end{bmatrix} = \begin{bmatrix} 0 & \mathcal{J} & 0 \\ -\mathcal{J}^\top & 0 & -\mathcal{G} \\ 0 & \mathcal{G}^\top & -\Lambda_\xi \end{bmatrix} \begin{bmatrix} \left( \frac{\partial \bar{\mathcal{H}}_d}{\partial \mathbf{r}} \right)^\top \\ \left( \frac{\partial \bar{\mathcal{H}}_d}{\partial \rho} \right)^\top \\ \left( \frac{\partial \bar{\mathcal{H}}_d}{\partial \xi} \right)^\top \end{bmatrix} + \begin{bmatrix} 0 \\ \mathcal{J}^\top b \\ 0 \end{bmatrix} \lambda_d, \quad (3.26a)$$

$$0 = b^\top \mathcal{J} \left( \frac{\partial \bar{\mathcal{H}}_d}{\partial \rho} \right)^\top, \quad (3.26b)$$

$$\bar{\mathcal{H}}_d(\mathbf{r}, \rho) = \underbrace{\frac{1}{2} \rho^\top \mathcal{M}_d^{-1} \rho + \frac{1}{2} \psi^\top K_\psi \psi + \bar{\mathbf{r}}^\top b^* \mu^*}_{\mathcal{H}_d} + \frac{1}{2} \tilde{\xi}^\top \bar{K}_u \tilde{\xi}, \quad (\text{Hamiltonian})$$

where  $\tilde{\xi} = \xi + \bar{\psi}$ . Afterwards, the time derivative of the desire energy function

$$\dot{\bar{\mathcal{H}}}_d(\mathbf{r}, \rho) = -\frac{1}{2} \tilde{\xi}^\top \bar{K}_u^\top (\Lambda_\xi + \Lambda_\xi^\top) \bar{K}_u \tilde{\xi} \leq 0$$

reveals that  $\bar{\mathcal{H}}$  is a (weak) Lyapunov function. Therefore, invoking Barbashin-Krasovskii-Lasalle,  $\tilde{\xi}$  goes to zero as time goes to infinity. Eventually, if  $\tilde{\xi} = 0$  we return to the original desire implicit structure, i.e., (3.26) reduces to (3.3) with  $\mathcal{W} = 0$ ,

$\mathcal{G}^\top \mathcal{M}_d^{-1} \rho = 0 \equiv y_n$ . Asymptotical stability can be shown if (3.3) has a zero state detectable output  $y_n$ .  $\square$

**Remark.** *The condition  $\mathcal{J}^\top b = bk$  can also be stated as*

$$0 = b^\perp \mathcal{M} \left( (b^{*\perp})^\top A b^{*\perp} + Z_c D Z_c^\top \right) b, \quad (3.27)$$

*replacing (3.20b).*

---

## Chapter 4

# Explicit and Implicit IDA-PBC applied to a Portal Crane

---

In this chapter, it is presented the implementation of the explicit and implicit IDA-PBC approaches in a portal crane<sup>9</sup> system, whose main task consists of moving a payload in a smooth path and deposit the payload at the desired position. It is not a big surprise to find within the scope a vast literature with different linear and non-linear control approaches for this system [11, 15, 17, 19, 45–47]. However, the motivation for this system is in its relative complexity which becomes a valuable resource to show the advantages and disadvantages of the implicit non-linear controller. This chapter starts by describing the system in Section 4.1. Then in Section 4.2 and Section 4.3, we analyze, simulate and implement the IDA-PBC control laws in the real setup located at the Laboratory of Control Engineering Group at Computer Science and Automation Department, *Technische Universität Ilmenau*.

### 4.1 The Portal Crane System

Cranes are widely used in transportation and construction. Commonly they consist of a hoisting mechanism (traditionally a hoisting line and hook) and a support mechanism (trolley-girder) [6]. There are three classifications of the cranes: the portal crane, the rotary crane and the boom crane. The main difference between them lies on the degrees of freedom the support mechanism offers to the suspension point.

This work focuses on the portal crane system shown in Figure 4.1. Here, the support mechanism (frame) is attached to the floor, i.e., not all the portal crane moves. In the top, there are a set of girders and belts that move a bridge (Figure 4.1.b) through the  $x$ -axis motor. Meanwhile, the trolley is mounted under the bridge, and its movement is

---

<sup>9</sup>also known as gantry crane or overhead crane.

#### 4. Explicit and Implicit IDA-PBC applied to a Portal Crane

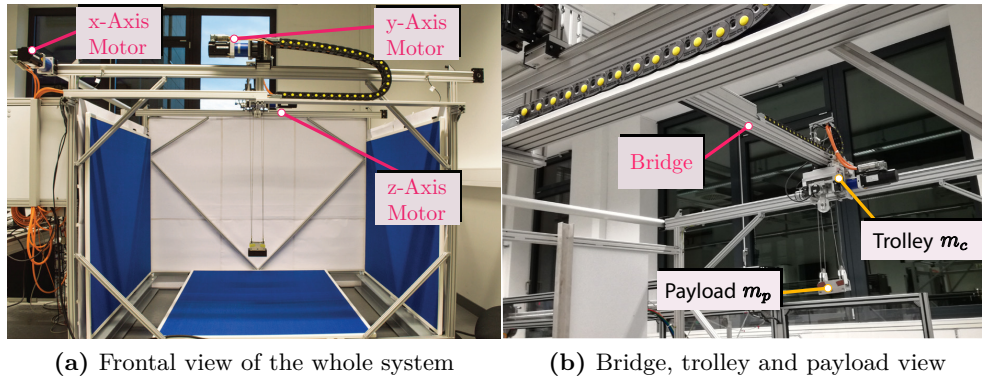


Figure 4.1. – Subfigures showing the portal crane system at the laboratory.

restricted to the  $y$ -direction. The  $x$ -axis,  $y$ -axis and  $z$ -axis motors are fixed in the frame, bridge and trolley, respectively. A sketch of this configuration is presented in Figure 4.2, where also, the frame dimensions are drawn. The maximum displacements of the trolley in each axis are drawn in brackets, e.g. for the  $x$ -axis is  $[0 - 2000]$ , where 0 represents the origin. It is clear that the displacements should be less than the frame dimensions.

A closer look of the trolley in Figure 4.3 shows other elements such as encoders, a pulley, and a winch or rope drum. A basket hangs from this winch, and thus it can also move in the  $z$ -direction. The load can be attached to the basket in various ways and then transported with it. We will refer to the basket and the additional weight (load) as the payload. Gravity produces a constant force on the payload. For this reason a driver must be equipped with a holding brake, preventing the payload movement (in

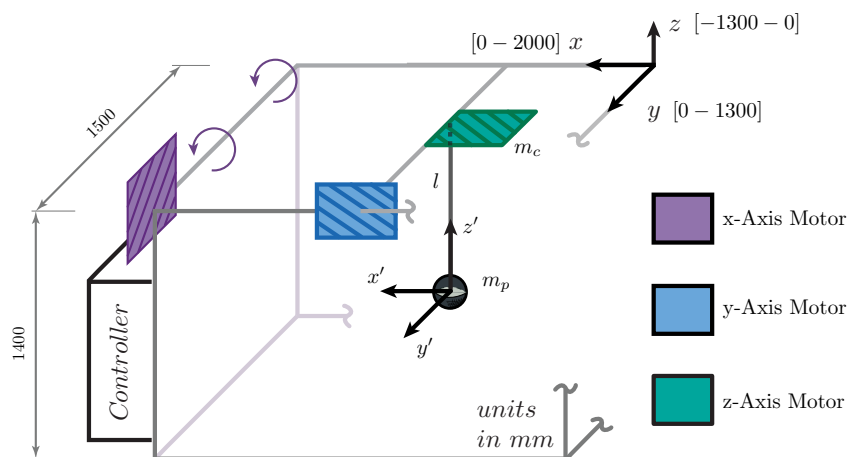
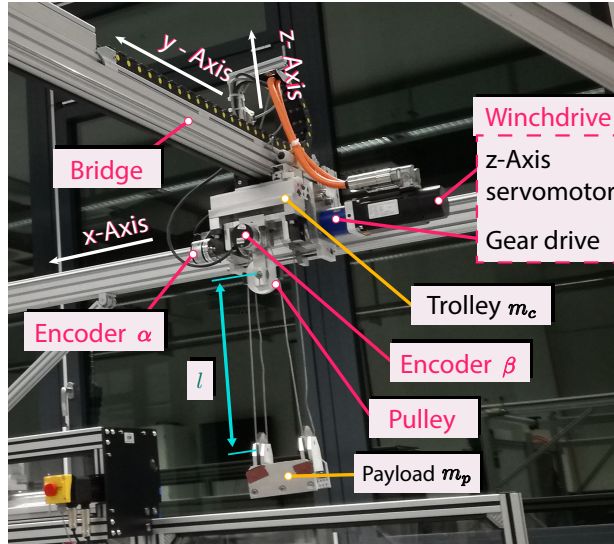


Figure 4.2. – Sketch of the portal crane.

the  $z$ -axis) without the servomotor being controlled. In case of failure, it also prevents the free fall of the payload to the ground.



**Figure 4.3.** – Trolley and its elements

#### 4.1.1 Additional Information of the Crane

Certainly, an advantage of this underactuated mechanical system is that it can be modelled in 2-D or 3-D space as we will see in Sections 4.2 and 4.3. Regardless of the model the goal is clear: To move the hanging load from one stationary position to a new, target. However, it is crucial to be aware of how the components achieve this goal. The physical setup is composed of a PC, a DS1103 controller board by the dSPACE company [48], actuators, sensors, and the trolley and pendulum. The Laboratory uses a fast prototyping approach. In essence, a full model of the system is built and simulated in the PC before a hardware implementation is generated. Thus, the computer is equipped with Matlab/Simulink and an RTI-toolbox, which compiles and export the algorithm to the controller. The controller is connected to the servo drivers who enables the control of the motor. There are two options to control them **(i)** by means of an internal velocity loop or **(ii)** through a current control that could be approximate to force control. However, the equipment do not have a sensor to measure the force applied to the  $x$ - or  $y$ -axis. Thus, implementing a force control would require many unknown parameters, e.g. the weights of the trolley, bridge, motors and other measurements in the encoders. To avoid this, we use option **(i)** which is almost equivalent to the PFL approach, where is usual to take as new input the acceleration of the system, see [49]. Thus, we can integrate the acceleration in order to use the velocity loop.

#### 4. Explicit and Implicit IDA-PBC applied to a Portal Crane

Let us remark, that the system is equipped with encoders (see Fig. 4.4a) to measure the angles  $\alpha(t)$  and  $\beta(t)$ . Moreover, the system is able to calculate the measurement of the trolley positions  $x_c(t)$  and  $y_c(t)$ . Besides, the positions of the payload are  $x_p(t)$ ,  $y_p(t)$  and  $z_p(t)$ , where the geometric restriction shown in Fig. 4.4b shows that

$$x_p = l \sin \beta, \quad y_p = l \cos \beta \sin \alpha, \quad z_p = l \cos \beta \cos \alpha$$

The velocities of the angles  $\dot{\alpha}$ ,  $\dot{\beta}$  and positions  $\dot{x}_c$ ,  $\dot{y}_c$  can also be measured through the encoders. Thus, the velocities of the generalized coordinates can be easily computed if we realized that each one can be defined as a function of the angles, and then the time derivative of each can be computed, e.g.,  $x_p = f(\beta) \rightarrow \frac{df(\beta)}{dt} = \frac{\partial f(\beta)}{\partial \beta} \dot{\beta}$ . Figure 4.5 illustrates the interconnection among the devices. The DS1103 specification are shown in Table 4.1.

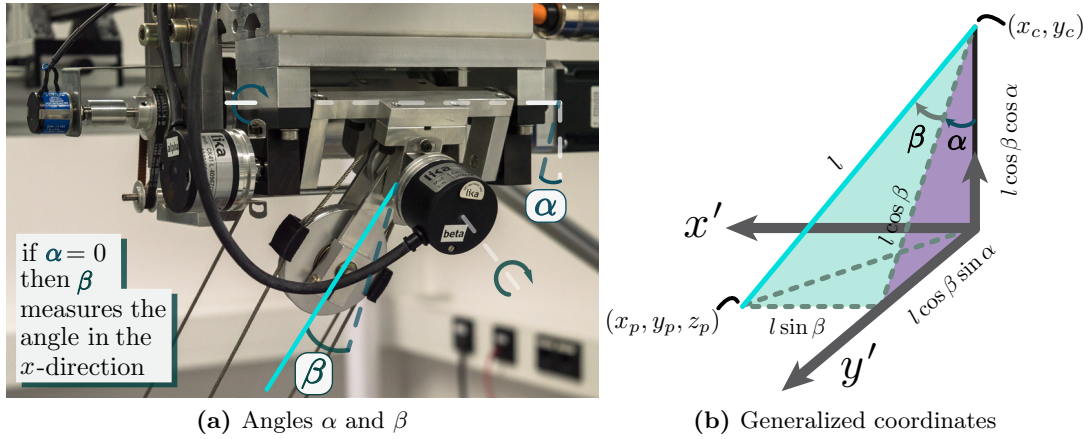


**Figure 4.4.** – Subfigures showing the relationship between the angles and the generalized coordinates

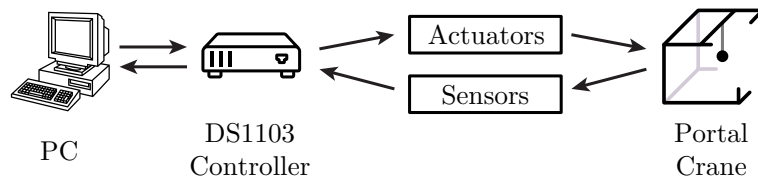


**Figure 4.5.** – PC, dSPACE and Portal Crane

#### 4.1.2 2-D Explicit Model

Before implementing the classical (explicit) IDA-PBC in an UMS, it is required first, to model the system dynamics, using, e.g., Newton-Euler or Euler-Lagrange equations,

#### 4. Explicit and Implicit IDA-PBC applied to a Portal Crane

DS1103	
Processor	933 MHz
I/O Channels	50 Bit - I/O Channels
A/D Channels	36
D/A Channels	8

**Table 4.1.** – Controller Board Specifications

and then, represent the system in port-Hamiltonian structure. The mathematical 2-D model for the crane is given by [50] and represented in Figure 4.6. Where  $m_c$  is the mass of the trolley,  $m_p$  is the mass of the payload,  $x_c$  denotes the trolley displacement<sup>10</sup>,  $l$  is the length of the rope,  $\beta$  is the payload swing angle w.r.t the vertical,  $F$  is the resultant force imposed on the trolley,  $f_r$  is the forced caused by the girder friction and  $g_r$  is the gravity force.

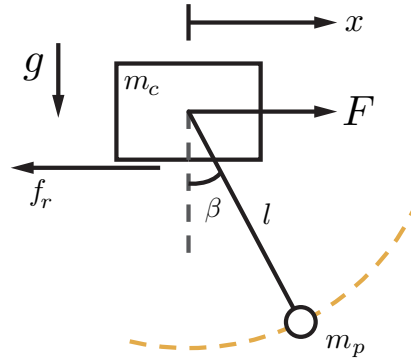


**Figure 4.6.** – 2-D crane

**Assumption 3.** *The payload is always under the trolley in the sense that*

$$-\frac{\pi}{2} < \beta < \frac{\pi}{2} \quad \forall t \geq 0. \quad (4.1)$$

Neglecting the friction, the dynamics of the system are described by

$$(m_c + m_p)\ddot{x}_c + m_p l \ddot{\beta} \cos(\beta) - m_p l \dot{\beta}^2 \sin(\beta) = F, \quad (4.2a)$$

$$m_p l^2 \ddot{\beta} + m_p l \cos(\beta)\ddot{x}_c + m_p l g_r \sin(\beta) = 0, \quad (4.2b)$$

<sup>10</sup>Note that it is possible to measure the displacement of the trolley in the  $y$ -axis, that is  $y_c$ . If so the angle to be considered w.r.t. the vertical is  $\alpha$ .



---

#### 4. Explicit and Implicit IDA-PBC applied to a Portal Crane

---

Let us divide (4.2) by  $m_p l^2$  and define  $\bar{g} := g_r/l$ ,  $a := 1/l$ ,  $\bar{m} := \frac{m_c+m_p}{m_p l^2}$  and  $\bar{F} := \frac{F}{m_p l^2}$ . Thus, we can represent (4.2) in compact form

$$\begin{bmatrix} 1 & a \cos \beta \\ a \cos \beta & \bar{m} \end{bmatrix} \begin{bmatrix} \ddot{\beta} \\ u \end{bmatrix} + \begin{bmatrix} 0 \\ -a\dot{\beta}^2 \sin \beta \end{bmatrix} + \begin{bmatrix} \bar{g} \sin \beta \\ 0 \end{bmatrix} = \begin{bmatrix} 0 \\ 1 \end{bmatrix} \bar{F} \quad (4.3)$$

Is possible to extend (4.3) to the pH structure [1] by using the partial feedback linearization method (see [49]) and taking

$$\bar{F} = \bar{m} u - a^2 \cos^2 \beta u - a \dot{\beta}^2 \sin \beta - a \bar{g} \sin \beta \cos \beta,$$

where the new input is the acceleration  $u = \ddot{x}_c$ . Thus, we are able to represent (4.3) as

$$I_2 \begin{bmatrix} \ddot{\beta} \\ \ddot{x}_c \end{bmatrix} = \begin{bmatrix} -\bar{g} \sin \beta \\ 0 \end{bmatrix} + \begin{bmatrix} -a \cos \beta \\ 1 \end{bmatrix} u, \quad (4.4)$$

where  $q = [q_1^\top \ q_2^\top]^\top = [\beta^\top \ x_c^\top]^\top$  are the generalized coordinates. To represent (4.4) in pH structure it is essential to recognize the mass matrix and the potential energy. Due to the partial feedback linearization, the mass matrix is now  $M = I_2$  and the linear momenta become equal to the time derivative of the generalized coordinates, that is  $\dot{\mathbf{q}} = M^{-1} \mathbf{p} = \mathbf{p}$ . The potential energy is calculated from  $-\partial V/\partial q_1 = \bar{g} \sin q_1 \Rightarrow V(\mathbf{q}) = \bar{g} \cos q_1$ . Therefore the pH system representation is

$$\begin{bmatrix} \dot{\mathbf{q}} \\ \dot{\mathbf{p}} \end{bmatrix} = \begin{bmatrix} 0 & I \\ -I & 0 \end{bmatrix} \begin{bmatrix} (\frac{\partial H}{\partial \mathbf{q}})^\top \\ (\frac{\partial H}{\partial \mathbf{p}})^\top \end{bmatrix} + \underbrace{\begin{bmatrix} 0 \\ G(\mathbf{q}) \end{bmatrix}}_{G_u} \mathbf{u} \quad (4.5)$$

$$H(\mathbf{q}, \mathbf{p}) = \frac{1}{2} \mathbf{p}^\top M^{-1} \mathbf{p} + V(\mathbf{q}) \quad (\text{Hamiltonian})$$

with  $G_u^\top = [0 \ G^\top(\mathbf{q})]^\top$ , where  $G^\top(\mathbf{q}) = [-a \cos \beta \ 1]$ .

#### 4.1.3 3-D Implicit Model

Similar to the explicit case, to perform the implicit IDA-PBC approach, we obtain the 3-D implicit model of the portal crane (as presented in (3.1)) which is presented in Figure 4.7. Where  $m_c$  is the mass of the trolley,  $m_p$  is the mass of the payload,  $x_c$  and  $y_c$  denotes the trolley displacements, meanwhile  $x_p$ ,  $y_p$  and  $z_p$  denotes the pendulum displacements relative to the trolley,  $b\lambda$  is a constraint force,  $l$  is the length of the

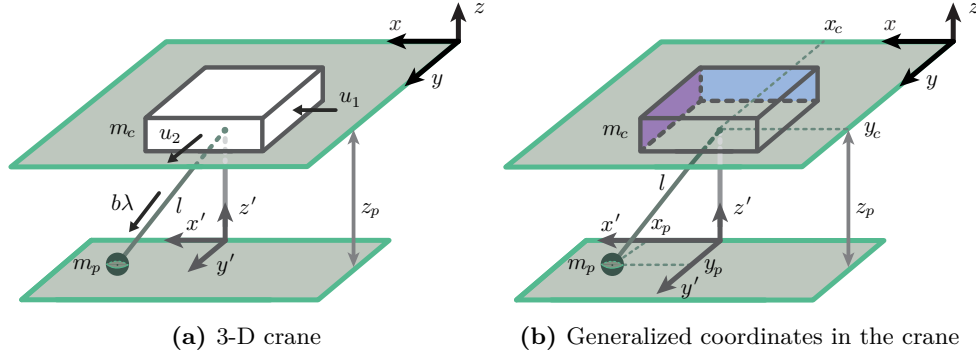


Figure 4.7. – Subfigures showing the portal crane 3-D model

rope<sup>11</sup>, and  $u_1, u_2$  are the trolley external forces imposed on the  $x$ - and  $y$ -axis. The generalized coordinates are  $\mathbf{r}^\top = [x_p \ y_p \ z_p \ x_c \ y_c]$ , and the constraint, resulting from a fixed rope length, can be selected as  $g(\mathbf{r}) := \frac{1}{2}(x_p^2 + y_p^2 + z_p^2 - l^2)$ .

The kinetic and the potential energy composes the Lagrangian, thus

$$T = \frac{1}{2} m_c (\dot{x}_c^2 + \dot{y}_c^2) + \frac{1}{2} m_p ((\dot{x}_c + \dot{x}_p)^2 + (\dot{y}_c + \dot{y}_p)^2 + \dot{z}_p^2) \quad (4.6)$$

and

$$\mathcal{V} = m_p g_r z_p. \quad (4.7)$$

The resulting Lagrange equations with external forces  $\mathcal{G} \mathbf{u}$  and constraints  $g(\mathbf{r}) = 0$  are

$$\frac{d}{dt} \left( \frac{\partial L}{\partial \dot{\mathbf{r}}} \right)^\top - \left( \frac{\partial L}{\partial \mathbf{r}} \right)^\top = b(\mathbf{r}) \boldsymbol{\lambda} + \mathcal{G} \mathbf{u}, \quad L = T - \mathcal{V}, \quad (4.8)$$

where  $b(\mathbf{r}) = (\partial g / \partial \mathbf{r})^\top$ ,  $\mathcal{G} = [0_{2 \times 3} \ I_2]^\top$ . According to (4.8), we have

$$\begin{bmatrix} M_1 & M_2 \\ M_2^\top & M_3 \end{bmatrix} \begin{bmatrix} \ddot{\mathbf{r}}_p \\ \ddot{\mathbf{r}}_c \end{bmatrix} = - \begin{bmatrix} (\frac{\partial \mathcal{V}}{\partial \mathbf{r}_p})^\top \\ (\frac{\partial \mathcal{V}}{\partial \mathbf{r}_c})^\top \end{bmatrix} + \begin{bmatrix} (\frac{\partial g}{\partial \mathbf{r}_p})^\top \\ (\frac{\partial g}{\partial \mathbf{r}_c})^\top \end{bmatrix} \boldsymbol{\lambda} + \begin{bmatrix} 0_{3 \times 2} \\ I_2 \end{bmatrix} \mathbf{u}, \quad (4.9)$$

where  $\mathbf{r}_p^\top = [x_p \ y_p \ z_p]$ ,  $\mathbf{r}_c^\top = [x_c \ y_c]$ ,  $\mathbf{u}^\top = [u_1 \ u_2]$ ,  $M_1 = m_p I_3$ ,  $M_2 = m_p \begin{bmatrix} I_2 \\ 0_{1 \times 2} \end{bmatrix}$  and  $M_3 = (m_c + m_p) I_2$ . As explained in Section 4.1.1 we need to use partial feedback

<sup>11</sup>It will be considered as a fixed value; otherwise, the constraint would not exist.

linearization. Setting as new input  $\mathbf{a}_c = \ddot{\mathbf{r}}_c$  (trolley acceleration), we obtain

$$I_5 \begin{bmatrix} \ddot{\mathbf{r}}_p \\ \ddot{\mathbf{r}}_c \end{bmatrix} = \begin{bmatrix} m_p^{-1} \left( \frac{\partial \mathcal{V}}{\partial \mathbf{r}_p} \right)^\top \\ 0 \end{bmatrix} + \begin{bmatrix} m_p^{-1} \left( \frac{\partial g}{\partial \mathbf{r}_p} \right)^\top \\ 0 \end{bmatrix} \boldsymbol{\lambda} + \underbrace{\begin{bmatrix} G_1 \\ I_2 \end{bmatrix}}_{\bar{\mathcal{G}}} \mathbf{a}_c, \quad (4.10)$$

where  $G_1 = -m_p^{-1} M_2$  and  $\check{\mathcal{M}} = I_5$  is the new mass matrix. Now, it is possible to represent the system in an implicit pH representation, that is

$$\begin{bmatrix} \dot{\mathbf{r}} \\ \dot{\boldsymbol{\rho}} \end{bmatrix} = \begin{bmatrix} 0 & I_5 \\ -I_5 & 0 \end{bmatrix} \begin{bmatrix} \left( \frac{\partial \check{\mathcal{H}}}{\partial \mathbf{r}} \right)^\top \\ \left( \frac{\partial \check{\mathcal{H}}}{\partial \boldsymbol{\rho}} \right)^\top \end{bmatrix} + \begin{bmatrix} 0 \\ b(\mathbf{r}) \end{bmatrix} \check{\boldsymbol{\lambda}} + \begin{bmatrix} 0 \\ \bar{\mathcal{G}} \end{bmatrix} \mathbf{a}_c, \quad (4.11a)$$

$$b^\top(\mathbf{r}) \frac{\partial \check{\mathcal{H}}}{\partial \boldsymbol{\rho}} = 0, \quad (4.11b)$$

$$\check{\mathcal{H}}(\mathbf{r}, \boldsymbol{\rho}) = \frac{1}{2} \boldsymbol{\rho}^\top \check{\mathcal{M}}(\mathbf{r})^{-1} \boldsymbol{\rho} + \check{\mathcal{V}}(\mathbf{r}), \quad (\text{Hamiltonian})$$

where  $\bar{\mathcal{G}}^\top = \begin{bmatrix} G_1^\top & I_2 \end{bmatrix}$ ,  $\check{\mathcal{V}} = g_r z_p$  is the new potential energy (taken from  $\frac{1}{m_p} \left( \frac{\partial \mathcal{V}}{\partial \mathbf{r}_p} \right)^\top \equiv \left( \frac{\partial \check{\mathcal{V}}}{\partial \mathbf{r}_p} \right)^\top$ ) and  $\check{\boldsymbol{\lambda}} = \frac{1}{m_p} \boldsymbol{\lambda}$  is the new implicit variable.

## 4.2 Explicit IDA-PBC Applied to the Portal Crane

We are now ready to present the steps to find a well-defined state feedback law from (4.5) of the 2-D crane model. As a reference, we follow the procedure of [1]. However, in that paper, the author has made a flaw while implementing the IDA-PBC method.

### 4.2.1 State feedback law from [1]

The desired closed-loop pH structure has the same form as in (2.40), that is

$$\begin{bmatrix} \dot{\mathbf{q}} \\ \dot{\mathbf{p}} \end{bmatrix} = \begin{bmatrix} 0 & J_1 \\ -J_1^\top & J_2 - R_2 \end{bmatrix} \begin{bmatrix} \left( \frac{\partial H^*}{\partial \mathbf{q}} \right)^\top \\ \left( \frac{\partial H^*}{\partial \mathbf{p}} \right)^\top \end{bmatrix}, \quad (4.12)$$

$$H^*(\mathbf{q}, \mathbf{p}) = \frac{1}{2} \mathbf{p}^\top M^*(\mathbf{q})^{-1} \mathbf{p} + V^*(\mathbf{q}), \quad (\text{Desired Energy Function})$$

where we pick a full rank left annihilator of  $G$ , that is  $G^\perp = \begin{bmatrix} 1 & -a \cos(q_1) \end{bmatrix}$  it is clear that the desired mass matrix has the following form

$$M^*(\mathbf{q}) = \begin{bmatrix} m_1(\mathbf{q}) & m_2(\mathbf{q}) \\ m_2(\mathbf{q}) & m_3(\mathbf{q}) \end{bmatrix}. \quad (4.13)$$

---

#### 4. Explicit and Implicit IDA-PBC applied to a Portal Crane

---

Then, the potential energy matching condition (2.44b) results in

$$(-a m_2 \cos(q_1) - m_1) \frac{\partial V^*(\mathbf{q})}{\partial q_1} + (-a m_3 \cos(q_1) - m_2) \frac{\partial V^*(\mathbf{q})}{\partial q_2} + \bar{g} \sin(q_1) = 0. \quad (4.14)$$

To reduce the complexity of (4.14), it is possible to choose  $m_2 = -m_3 a \cos(q_1)$ ; thus, (4.14) is a simple integral in  $q_1$  that can be solved, e.g in Maple, and results in

$$V^*(\mathbf{q}) = \frac{-\bar{g} \operatorname{arctanh}\left(\frac{a m_3 \cos(q_1)}{\sqrt{m_1 m_3}}\right)}{a \sqrt{m_1 m_3}} + \Upsilon(q_2), \quad (4.15)$$

where  $\Upsilon(q_2)$  is an arbitrary differentiable function s.t  $q^* = \arg \min V^*(\mathbf{q})$  is an isolated minimum. By taking  $\Upsilon(q_2) = 1/2 K_p (q_2 - q_2^*)^2$ , the necessary and sufficient conditions for  $V^*$  to possess a local strict minimum in  $\mathbf{q}^* = (0, q_2^*)$  are

$$\left. \frac{\partial V^*}{\partial \mathbf{q}} \right|_{\mathbf{q}^*} = 0, \quad \left. \frac{\partial^2 V^*}{\partial \mathbf{q}^2} \right|_{\mathbf{q}^*} = \begin{bmatrix} -\frac{\bar{g}}{a^2 m_3 - m_1} & 0 \\ 0 & K_p \end{bmatrix} \succ 0. \quad (4.16)$$

The matrix in the second condition is clearly positive definite picking  $m_1 = m_3 a^2 + \varepsilon$ ,  $\varepsilon > 0$  and  $K_p > 0$ . Now the shaped energy function is

$$V^*(\mathbf{q}) = \frac{-\bar{g} \operatorname{arctanh}\left(\frac{a m_3 \cos(q_1)}{\sqrt{m_3 (a^2 m_3 + \varepsilon)}}\right)}{a \sqrt{m_3 (a^2 m_3 + \varepsilon)}} + \frac{1}{2} K_p (q_2 - q_2^*)^2, \quad (4.17)$$

and

$$M^*(\mathbf{q}) = \begin{bmatrix} a^2 m_3 + \varepsilon & -a m_3 \cos q_1 \\ -a m_3 \cos q_1 & m_3 \end{bmatrix}. \quad (4.18)$$

Next step is to solve the matching condition related to the kinetic energy, i.e., (2.44a).

By taking  $J_2 = \begin{bmatrix} 0 & j_2 \\ -j_2 & 0 \end{bmatrix}$  it results in

$$j_2 = \frac{a m_3 \sin(q_1) (p_1 1 + (p_2 a \cos(q_1)) ((a m_3 p_1 \cos(q_1)) + p_2 (a^2 m_3 + \varepsilon)))}{p_2 (a^2 m_3 \cos^2(q_1) - a^2 m_3 - \varepsilon)} \quad (4.19)$$

However, taking (4.19) and trying to implement the control law  $\mathbf{u}_{ida}$ , defined by (2.42), will lead to the mistake of [1]. First, the matching condition (2.44a) is not satisfied whenever the momenta  $p_2 = 0$ , and second,  $\mathbf{u}_{ida}$  has  $p_2$  in its denominator; thus, the closed-loop is not well-defined for all  $(\mathbf{r}, \boldsymbol{\rho}) \in \{(\mathbf{r}, \boldsymbol{\rho}) \mid p_2 = 0\}$ .

### 4.2.2 A well-defined state feedback law using IDA-PBC

To avoid the aforementioned problems, we find different  $M^*$  and  $V^*$ . The starting point is to take a look at the skew symmetric property of  $J_2$

$$\frac{\partial H^*}{\partial \mathbf{p}} J_2 \left( \frac{\partial H^*}{\partial \mathbf{p}} \right)^\top = 0. \quad (4.20)$$

Now define

$$h := \frac{\partial H^*}{\partial \mathbf{p}} = \dot{\mathbf{q}}^\top J_1^{-\top} = \begin{bmatrix} h_1 & h_2 \end{bmatrix}, \quad J_2 := \begin{bmatrix} 0 & -s \\ s & 0 \end{bmatrix} h^\top \begin{bmatrix} 1 & \bar{b} \end{bmatrix},$$

with  $s$  an arbitrary function of  $\mathbf{q}$ . Replacing them in (2.44a) results in

$$G^\perp \left( -J_1^\top \left( \frac{\partial \mathbf{p}^\top M^*(\mathbf{q})^{-1} \mathbf{p}}{\partial \mathbf{q}} \right)^\top + 2 \begin{bmatrix} 0 & -s \\ s & 0 \end{bmatrix} h^\top \begin{bmatrix} 1 & \bar{b} \end{bmatrix} \left( \frac{\partial H^*}{\partial \mathbf{p}} \right)^\top \right) = 0. \quad (4.21)$$

Using the identity

$$\left( \frac{\partial \mathbf{p}^\top M^*(\mathbf{q})^{-1} \mathbf{p}}{\partial \mathbf{q}} \right)^\top = - \sum_{k=1}^2 e_k \mathbf{p}^\top M^{*-1} \frac{\partial(M^*)}{\partial q_k} M^{*-1} \mathbf{p},$$

in (4.21), where  $e_k$  represents the unit column vector of size 2, i.e., the  $k$ -th column of the identity matrix  $I_2$ , gives

$$G_\perp J_1 \sum_{k=1}^2 e_k \begin{bmatrix} h_1 & h_2 \end{bmatrix} \frac{\partial(M^*)}{\partial q_k} \begin{bmatrix} h_1 \\ h_2 \end{bmatrix} + 2 G_\perp \begin{bmatrix} 0 & -s \\ s & 0 \end{bmatrix} \begin{bmatrix} h_1 \\ h_2 \end{bmatrix} (h_1 + \bar{b} h_2) = 0. \quad (4.22)$$

Now, if we pick  $\bar{b} = 0$ ,

$$M^*(\mathbf{q}) = M^*(q_1) = \begin{bmatrix} m_1(q_1) & m_2(q_1) \\ m_2(q_1) & m_3 \end{bmatrix},$$

and define

$$K := G_\perp J_1 = \left[ \underbrace{m_1(q_1) + a m_2(q_1) \cos(q_1)}_{K_1} \quad \underbrace{m_2(q_1) + a m_3 \cos(q_1)}_{K_2} \right]. \quad (4.23)$$

Equation (4.22) becomes

$$\begin{aligned}
0 &= K \sum e_k \begin{bmatrix} h_1 & h_2 \end{bmatrix} \frac{\partial(M^*)}{\partial q_k} \begin{bmatrix} h_1 \\ h_2 \end{bmatrix} + 2 G_\perp \begin{bmatrix} 0 & -s \\ s & 0 \end{bmatrix} \begin{bmatrix} h_1 \\ h_2 \end{bmatrix} h_1, \\
&= K_1 \left( h_1^2 \frac{\partial m_1(q_1)}{\partial q_1} + 2 h_1 h_2 \frac{\partial m_2(q_1)}{\partial q_1} \right) + 2 h_1 \begin{bmatrix} 1 & a \cos(q_1) \end{bmatrix} \begin{bmatrix} -s h_2 \\ s h_1 \end{bmatrix}, \\
&= h_1^2 K_1 \frac{\partial m_1(q_1)}{\partial q_1} + 2 h_1 h_2 K_1 \frac{\partial m_2(q_1)}{\partial q_1} + h_1^2 2 a s \cos(q_1) - 2 h_1 h_2 s, \\
&= h_1^2 \left( K_1 \frac{\partial m_1(q_1)}{\partial q_1} + 2 a s \cos(q_1) \right) + 2 h_1 h_2 \left( K_1 \frac{\partial m_2(q_1)}{\partial q_1} - s \right). \quad (4.24)
\end{aligned}$$

Then, the only possible solution of (4.24) for arbitrary  $h_1$  and  $h_2$  is that in the last equality both terms in parenthesis are equal to zero. We select, as before,  $m_2(q_1) = -a m_3 \cos(q_1)$  to simplify the potential energy PDE and proceed to calculate  $s$  from the term that multiplies  $2 h_1 h_2$ , obtaining

$$s = a m_3 \sin(q_1) K_1.$$

Then, from the term multiplying  $h_1^2$ , it follows that

$$K_1 \frac{\partial m_1(q_1)}{\partial q_1} = -2 a s \cos(q_1) \quad \Rightarrow \quad m_1(q_1) = \frac{1}{2} a^2 m_3 \cos(2 q_1) + c_1,$$

where  $c_1$  is an arbitrary constant. Thus, the new shaped mass matrix is

$$M^*(\mathbf{q}) = \begin{bmatrix} m_1(q_1) & m_2(q_1) \\ m_2(q_1) & m_3 \end{bmatrix} = \begin{bmatrix} \frac{1}{2} a^2 m_3 \cos(2 q_1) + c_1 & -a m_3 \cos(q_1) \\ -a m_3 \cos(q_1) & m_3 \end{bmatrix}. \quad (4.25)$$

As mentioned previously, replacing  $M^*(\mathbf{q})$  (with  $m_2(q_1) = -a m_3 \cos(q_1)$ ) in (2.44b), results in a simplification of the matching condition, that is

$$(a^2 m_3 \cos^2(q_1) - \frac{1}{2} a^2 m_3 \cos(2 q_1) - c_1) \frac{\partial V^*(\mathbf{q})}{\partial q_1} + \bar{g} \sin(q_1) = 0,$$

which is again an integral and can be computed with Maple to obtain

$$V^*(\mathbf{q}) = \frac{2 \bar{g} \cos(q_1)}{2 c_1 - a^2 m_3} + \Upsilon(q_2) \quad (4.26)$$

---

#### 4. Explicit and Implicit IDA-PBC applied to a Portal Crane

---

Eventually, the necessary and sufficient conditions for  $q^* = (0, q_2^*)$  to be a strict local minimum of  $V^*(\mathbf{q})$  with  $\Upsilon(q_2) := 1/2 K_p (q_2 - q_2^*)^2$ , are  $\frac{\partial V^*}{\partial \mathbf{q}} \Big|_{\mathbf{q}^*} = 0$  and

$$\frac{\partial^2 V^*}{\partial \mathbf{q}^2} \Big|_{\mathbf{q}^*} = \begin{bmatrix} -\frac{2\bar{g}}{a^2 m_3 - 2c_1} & 0 \\ 0 & K_p \end{bmatrix} \succ 0. \quad (4.27)$$

Inequality (4.27) is verified if  $K_p > 0$  and  $c_1 > a^2 m_3/2$ . Thus, it is possible to select  $c_1 = a^2 m_3$ . Finally, taking  $R_2 = G K_v G^\top$  where  $K_v$  is a positive scalar, and  $J_{20} = 0$ , i.e.,  $J_2 \equiv J_{21}$ , we see that the (explicit) IDA-PBC controller (2.42) is reduced to

$$u_{ida} = \frac{2 m_3 \sin(q_1) ((\bar{g} + a p_1 p_2) \cos(q_1) + p_1^2) - a (m_3^2 K_p (q_2 - q_2^*) + K_v p_2)}{a m_3}. \quad (4.28)$$

It is clear that the control law (4.28) is well defined for any  $p_2$ . Moreover, it is independent of the weights of the trolley and the pendulum  $m_c$  and  $m_p$ .

### 4.2.3 Results

The parameters for the following simulations are shown in Table 4.2 and Table 4.3. Figure 4.8 shows the block diagram of the system, where the input is the target position. As the real system has a velocity loop, the  $u_{ida}$  is integrated to obtain the desired velocity. The next block is the crane with partial feedback linearization, whose components are shown in Figure 4.9. Besides the state feedback, it needs the constants  $l$ ,  $g_r$ , the tuning parameter  $m_3$ , and the tuning values  $K_p$  and  $K_v$ . The measurement of  $p_1$  and  $p_2$  can be obtained thanks to the encoder and the controller (since  $\mathbf{p} = \dot{\mathbf{q}}$ ), see Section 4.1.1.

symbol	description	value	unit
$m_p$	payload mass	4.975	kg
$l$	rope length	1.00	m
$g_r$	gravitational constant	9.81	m/s <sup>2</sup>

**Table 4.2.** – Crane constant parameters

The implementation is made in the  $y$ -axis, where the system was at rest, i.e. initial velocities are zero. The measured angled in this direction was  $\alpha$ , see Figure 4.4a. Figure 4.10 show the portal crane response to a set point  $y_c^*$  that changes between 0, 0.2,  $-0.2$  and 0.4. Figure 4.11 shows the swing angle behaviour and Figure 4.12 illustrates the control law. It is easy to note that simulation and result measurement are quite similar. The response shows an asymptotically stable behaviour. However, due to uncertain parameters like the vibration of the frame, friction, and encoder lack

#### 4. Explicit and Implicit IDA-PBC applied to a Portal Crane

symbol	description	value	unit
$m_3$	constant in $M^*$	0.42	kg
$c_1$	constant in $V^*$	$a^2 m_3$	kg/m <sup>2</sup>
$K_v$	constant in $u_{ida}$	1.80	
$K_p$	constant in $u_{ida}$	15.00	

Table 4.3. – (Explicit) IDA-PBC tuning paramaters

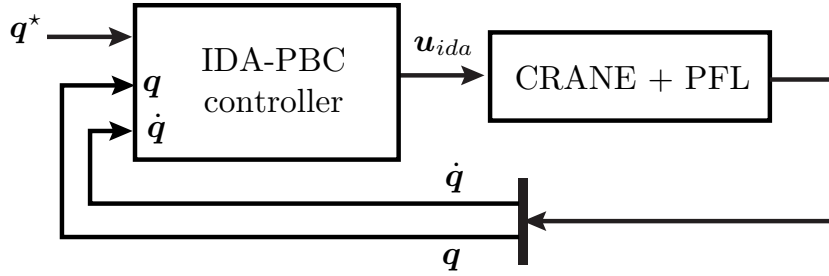


Figure 4.8. – (Explicit) IDA-PBC block diagram

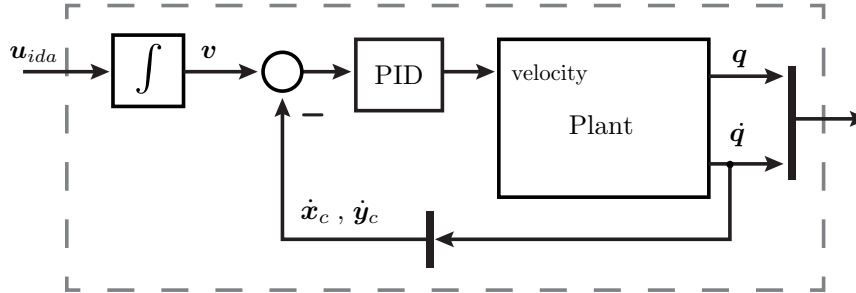


Figure 4.9. – Block crane plus partial feedback linearization (CRANE + PFL)

of resolution, we see some noise in the control law.

### 4.3 Implicit IDA-PBC Applied to the Portal Crane

We follow the algorithm steps in Figure 3.1 to obtain the implicit control law. Besides, considering the additional requirements it is possible to get a position feedback law. To close this section, we present the simulation and implementation results.



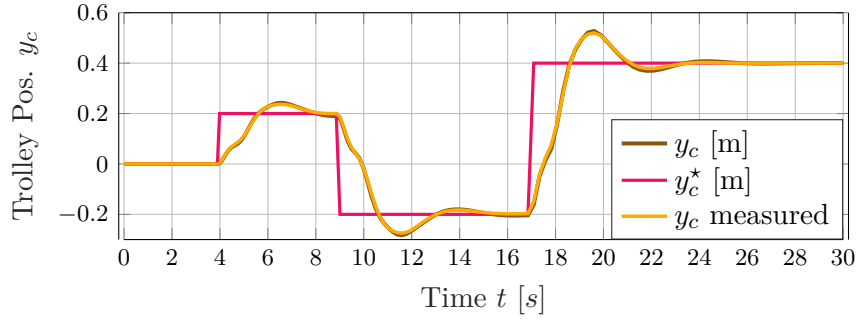


**Figure 4.10.** – Simulated and measured trolley displacement in  $y$ -axis

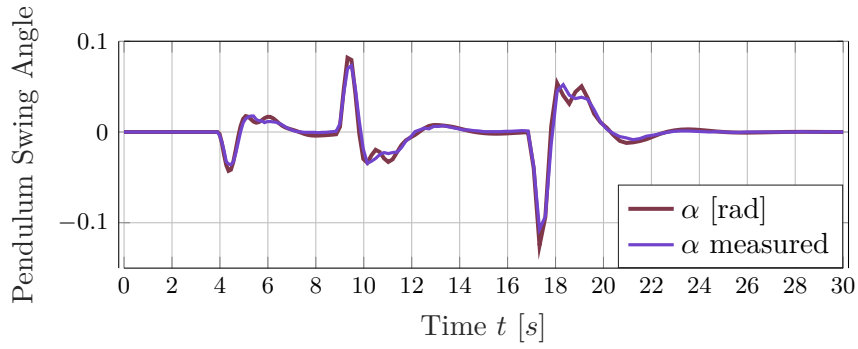


**Figure 4.11.** – Simulated and measured swing angle  $\alpha$  in the  $y$ -axis.  
Note that is assumed that  $\beta \equiv 0$

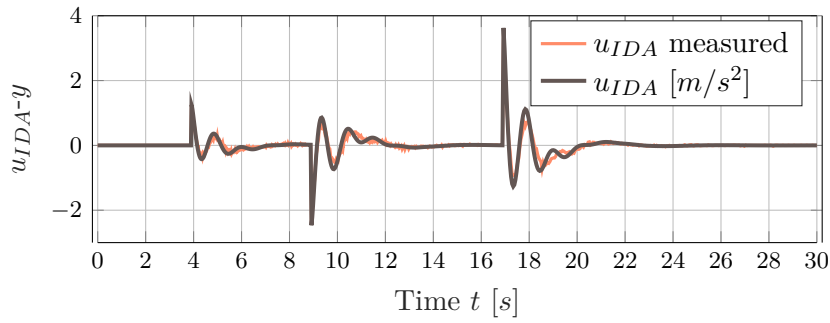


**Figure 4.12.** – Simulated (Explicit) IDA-PBC control law  $u_{IDA}$  applied in the  $y$ -direction and the measured control law

#### 4.3.1 State feedback law

We proceed to employ the algebraic IDA-PBC algorithm. We have already selected the coordinates and function  $g$ . Thus, the first step is to select  $\mathbf{r}^* = [0 \ 0 \ -l \ x_c^* \ y_c^*] \in \mathcal{X}_a$ , calculate  $\mathbf{b}(\mathbf{r}) = \left(\frac{\partial g}{\partial \mathbf{r}}\right)^\top = [x_p \ y_p \ z_p \ 0 \ 0]^\top$ ,  $\mathbf{b}^* = [0 \ 0 \ -l \ 0 \ 0]^\top$ ,  $\mathbf{S} = \begin{bmatrix} \bar{\mathbf{g}} & \mathbf{b} \end{bmatrix}$ , select the full

---

#### 4. Explicit and Implicit IDA-PBC applied to a Portal Crane

---

rank left annihilators

$$S^\perp = \begin{bmatrix} -z_p & 0 & x_p & -z_p & 0 \\ 0 & -z_p & y_p & z_p & 0 \end{bmatrix}, \quad (b^*)^\perp = \begin{bmatrix} I_2 & 0_{2 \times 1} & 0_2 \\ 0_2 & 0_{2 \times 1} & I_2 \end{bmatrix}$$

and define  $D_x := D l^2$ . Matrix  $Z_c$  can be reduced to  $b^*$  selecting  $C = 0_{4 \times 1}$ . From (3.20a) and (3.20b), we have

$$\begin{bmatrix} x_p(g_r - D_x l \mu^*) \\ y_p(g_r - D_x l \mu^*) \end{bmatrix} = \begin{bmatrix} 0 \\ 0 \end{bmatrix}, \quad (4.29)$$

$$\begin{bmatrix} ((a_{11} + a_{31}) l \mu^* - g_r) x_p + (a_{12} + a_{32}) l \mu^* y_p \\ (a_{21} + a_{41}) l \mu^* x_p + ((a_{22} + a_{42}) l \mu^* - g_r) y_p \end{bmatrix} = 0. \quad (4.30)$$

where  $a_{ij}$  is an element of  $A$  located in the  $i$ th row and  $j$ th column. Solving for arbitrary  $x_p$  and  $y_p$  with symmetric  $A$ , leads to  $D_x = \frac{g_r}{l \mu^*}$ ,  $a_{14} = a_{23}$ ,  $a_{14} = -a_{12}$ ,  $a_{31} = D_x - a_1$  and  $a_{42} = D_x - a_3$ . After renaming  $a_2 = a_{12}$ ,  $a_{11} = a_1$ ,  $a_{22} = a_3$ ,  $a_{33} = a_4$ ,  $a_{34} = a_{43} = a_5$  and  $a_{44} = a_6$ , matrix  $A$  has the following form

$$A = \begin{bmatrix} a_1 & a_2 & D_x - a_1 & -a_2 \\ a_2 & a_3 & -a_2 & D_x - a_3 \\ D_x - a_1 & -a_2 & a_4 & a_5 \\ -a_2 & D_x - a_3 & a_5 & a_6 \end{bmatrix}. \quad (4.31)$$

We might also consider the stronger condition<sup>12</sup>  $b^\perp J^\top b = 0$ , which results in  $a_2 = 0$  and  $a_1 = a_3 = D_x$ . Replacing them in (4.31), yields

$$A = \begin{bmatrix} D_x & 0 & 0 & 0 \\ 0 & D_x & 0 & 0 \\ 0 & 0 & a_4 & a_5 \\ 0 & 0 & a_5 & a_6 \end{bmatrix}.$$

With this  $A$ , (3.21) becomes

$$M_d = \begin{bmatrix} D_x & 0 & 0 & 0 & 0 \\ 0 & D_x & 0 & 0 & 0 \\ 0 & 0 & D_x & 0 & 0 \\ 0 & 0 & 0 & a_4 & a_5 \\ 0 & 0 & 0 & a_5 & a_6 \end{bmatrix}.$$

---

<sup>12</sup>We take this condition because it will be later used in Section 4.3.2. However, this condition reduces the tuning capabilities.

---

#### 4. Explicit and Implicit IDA-PBC applied to a Portal Crane

---

The next step is select  $\bar{S}$ . Since  $\bar{G}$  is constant, selecting  $S\bar{S} = \bar{G} \rightarrow \bar{S} = [I_2 \ 0_{2 \times 1}]^\top$  meets Equation (3.20c). Now it is possible to calculate the matrix  $Z$  and choose  $Z^\perp = \begin{bmatrix} 1 & 0 & 1 & 0 \\ 0 & 1 & 0 & 1 \end{bmatrix}$ . Then,  $W_1 = 0_{5 \times 5}$  is a valid selection for (3.23a). At this point, we are able to calculate  $\psi$ , that is

$$\psi = \begin{bmatrix} -\frac{x_p}{D_x} + \frac{a_6(x_c - x_c^*)}{a_6 a_4 - a_5^2} - \frac{a_5(y_c - y_c^*)}{a_6 a_4 - a_5^2} \\ -\frac{y_p}{D_x} + \frac{a_5(x_c - x_c^*)}{a_6 a_4 - a_5^2} + \frac{a_4(y_c - y_c^*)}{a_6 a_4 - a_5^2} \end{bmatrix}.$$

Using (3.20d) and (3.23b), the problem is reduced to select  $A \succ 0$ ,  $\mu^* > 0$ ,  $K_\psi \succ 0$  and  $K_u + K_u^\top \succ 0$ . Finally, all elements of the control law (3.6) are on hand.

#### 4.3.2 An output feedback law using the implicit IDA-PBC approach

As  $b^\perp J^\top b = 0$  and  $W_1 = 0$  hold, Proposition 5 can be used selecting  $A \succ 0$ ,  $K_\psi \succ 0$ ,  $\Lambda_\xi + \Lambda_\xi^\top \succ 0$  and symmetric  $\bar{K}_u \succ 0$ .

#### 4.3.3 Results

The parameters for the implicit IDA-PBC state feedback simulations are shown in Table 4.2 and Table 4.4. Figure 4.13 shows the block diagram of the system, where the input is the target position  $r^*$ . The block CRANE plus PFL is similar as the one shown in Figure 4.9 and thus avoided. Figure 4.14 shows the simulated system when  $x_c^*$  and

symbol	description	value
$a_4$	constant in $A$	82.5
$a_5$	constant in $A$	0
$a_6$	constant in $A$	62.5
$\mu^*$	constant in $D_x$	9.81/36
$K_u$	constant in $u_I$	80 diag(1.1, 1, 0)
$K_\psi$	constant in $u_I$	29 diag(0.9, 1)

**Table 4.4.** – Parameters for implicit state feedback IDA-PBC

$y_c^*$  are 0.8m. In the response, we can see a settling time of 12 seconds in the  $x$ -axis and 11 seconds in the  $y$ -axis; in both axis the maximum overshoot are minimal. However, it doesn't mean that is possible to find more suitable values to enhance the performance. Figure 4.15 and Figure 4.16 show the 3D crane response and controller behaviour, respectively, comparing it with the measured data. Responses achieve asymptotic stability. Besides, regarding some noise in the real control action, it is clear how it follows a similar path to the simulated one. The noise can be caused due to the vibration of

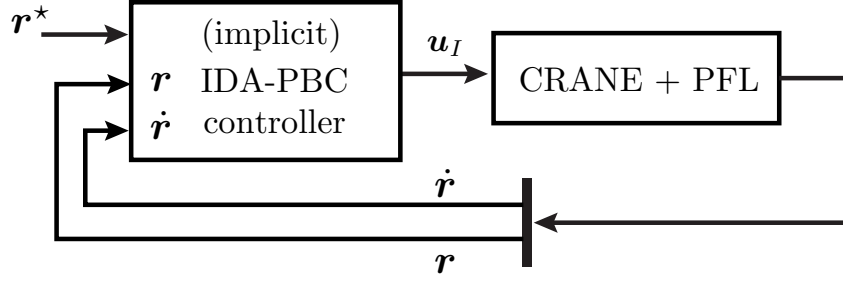


Figure 4.13. – Implicit algebraic IDA-PBC block diagram

the frame, and the lack of accuracy in the encoders. The positions of the pendulum are derived from the angles and the length of the rope. In this case, the angles velocities  $\dot{\alpha}$  and  $\dot{\beta}$  are measured thanks to the encoders and the generalized coordinates are computed as explained in Section 4.1.1.

The parameters for the implicit IDA-PBC output-feedback simulations are shown in Table 4.2 and Table 4.5. Figure 4.17 displays the block diagram of the system, where the input is the target position  $\mathbf{r}^*$  and the feedback is only  $\mathbf{r}$ . Figure 4.18 shows the inner elements of the implicit output-feedback controller where it requires to calculate  $\dot{\xi}$  using (3.25b).

Figure 4.19 show the response of the crane using the output-feedback controller (3.25)

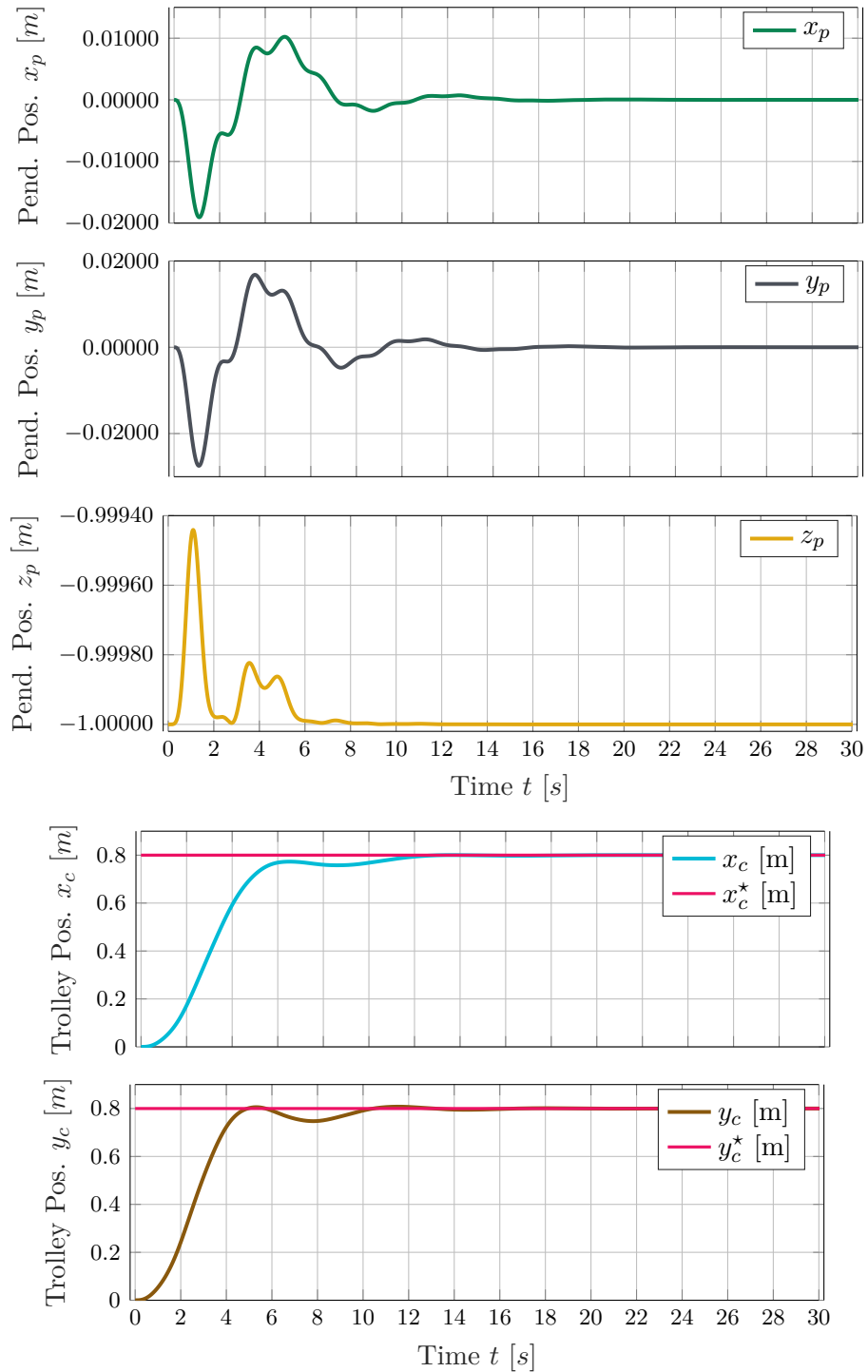
symbol	description	value
$a_4$	constant in $A$	29
$a_5$	constant in $A$	0
$a_6$	constant in $A$	29
$\mu^*$	constant in $D_x$	9.81/12
$\Lambda_\xi$	constant in $u_N$	$0.10I_2$
$\bar{K}_u$	constant in $u_N$	$175I_2$
$K_\psi$	constant in $u_N$	$0.0045I_2$

Table 4.5. – Parameters for implicit output-feedback IDA-PBC

and compares it with the measured data. It is easy to note that this approach guarantees asymptotic stability without overshooting and settling time of 9 and 10 seconds in  $x$ - and  $y$ -axis. It is also possible to see a constant error in the measurement of the trolley position  $x_c$ , due to lack of accuracy in the encoder. The behaviour of the output-feedback control law is shown in Figure 4.21. We can see a reduction of the noise since we don't measure the velocities.

We see great flexibility of using the implicit IDA-PBC approach. Compared to the explicit one, the advantage is to avoid the PDE, and moreover without difficulties to

#### 4. Explicit and Implicit IDA-PBC applied to a Portal Crane



**Figure 4.14.** – Simulation with state-feedback law  $u_I$  for desire  $x_c$  and  $y_c$

achieve the energy shaping. The (explicit) IDA-PBC was implemented successfully to the Portal Crane in 2-D and simulations show the results of the (explicit) controller

#### 4. Explicit and Implicit IDA-PBC applied to a Portal Crane

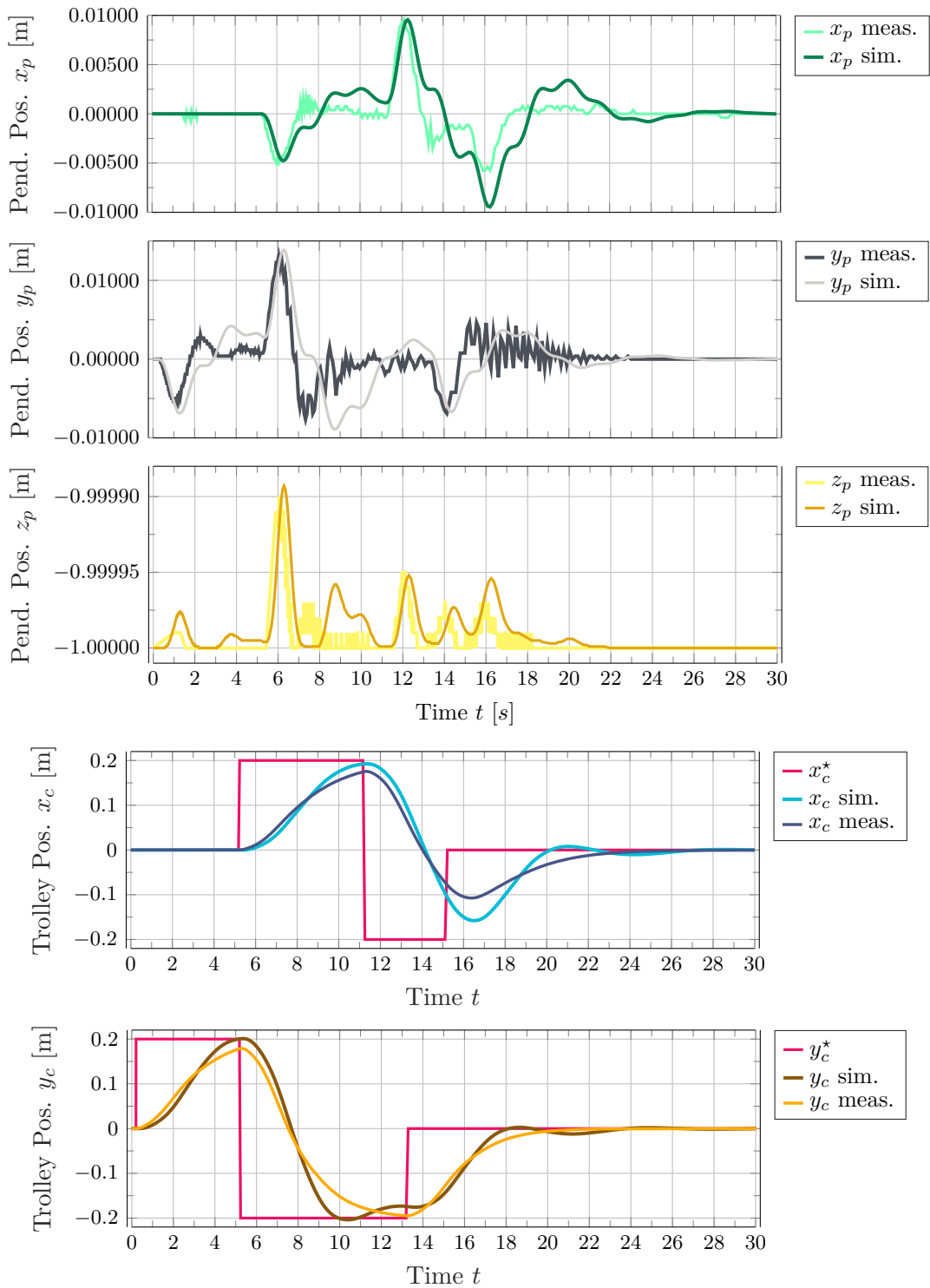


**Figure 4.15.** – Implementation implicit IDA-PBC and response of  $r$

#### 4. Explicit and Implicit IDA-PBC applied to a Portal Crane

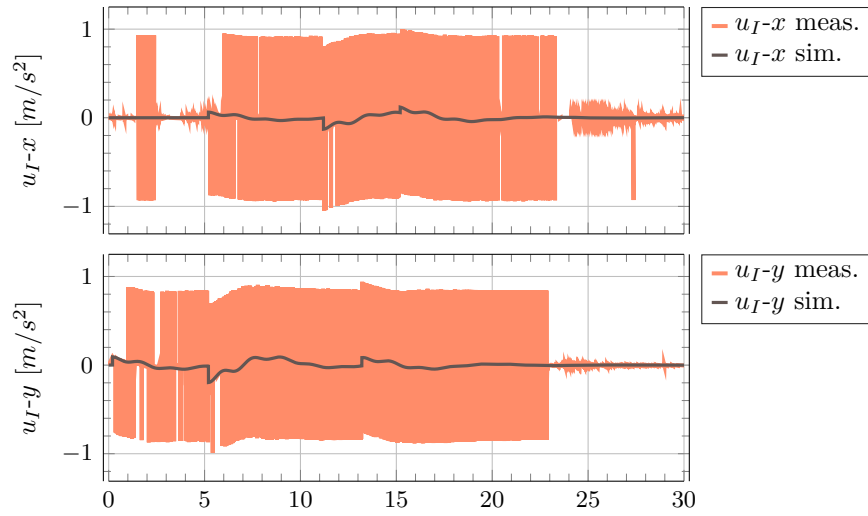


Figure 4.16. – Implicit control law  $u_I$

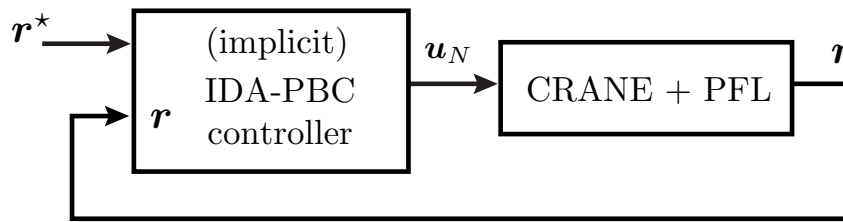


Figure 4.17. – Implicit Output-feedback IDA-PBC applied to the Portal Crane Block Diagram

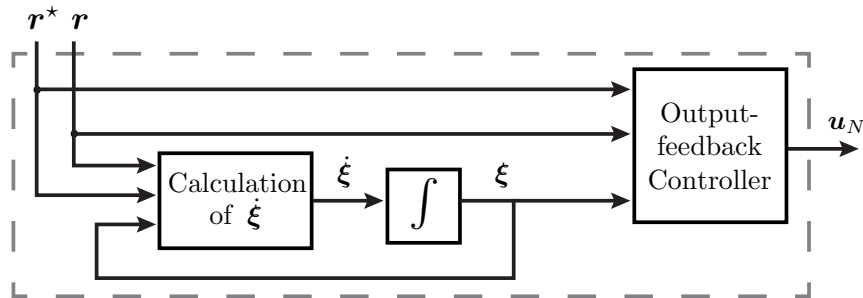
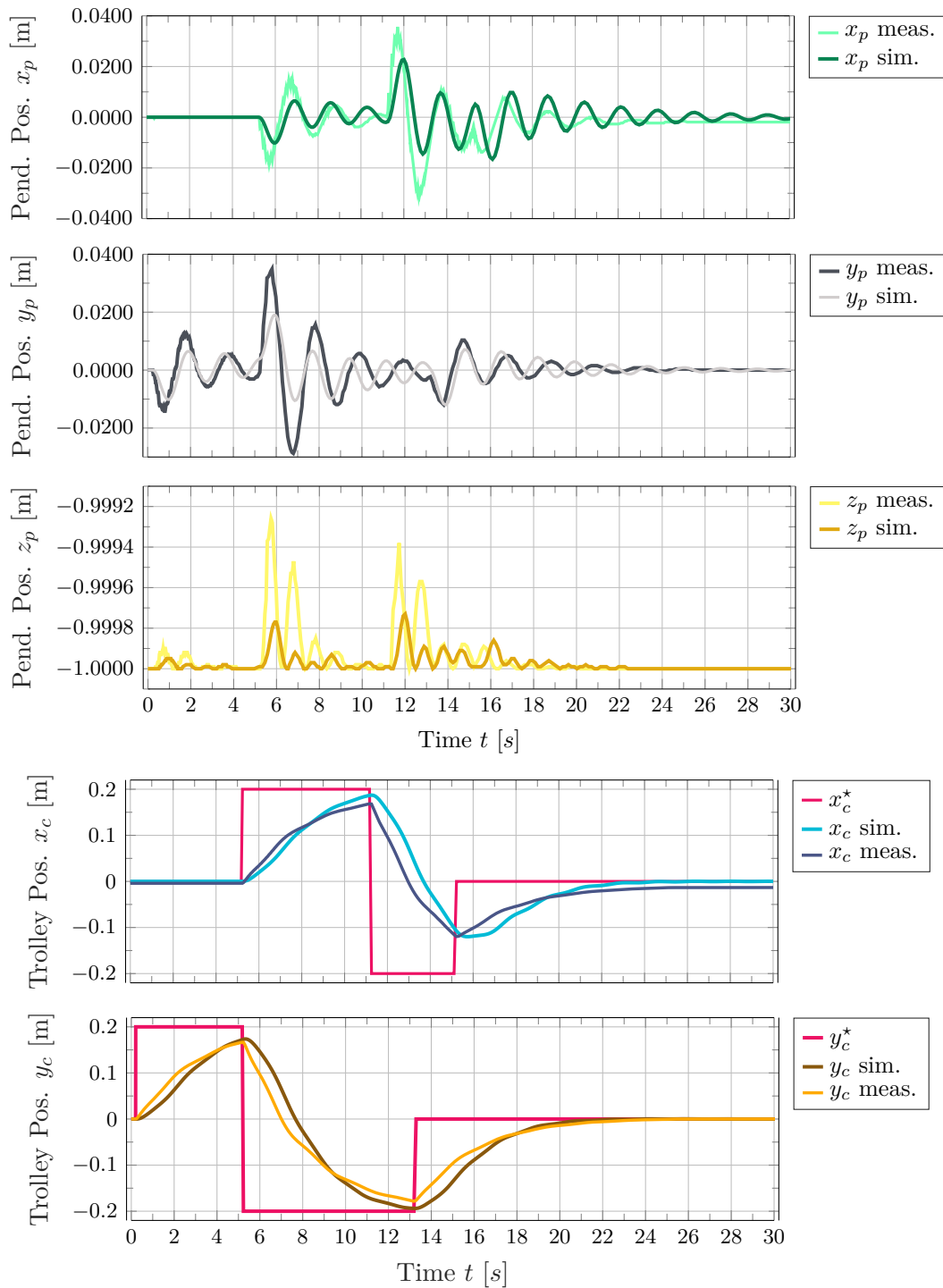


Figure 4.18. – Implicit Output-feedback IDA-PBC controller diagram

when the crane moves in the  $x$ -axis. However, we witnessed that the solution for a well-defined controller is not an easy task and in this case, lies in a mathematical move which simplifies the PDEs. Let us remark, that it is possible to apply the same (explicit) control law (4.28) in each axis  $x$  and  $y$ , to obtain complete control of the workspace.

#### 4. Explicit and Implicit IDA-PBC applied to a Portal Crane



**Figure 4.19.** – Output-feedback measurement

However, its performance can be affected since it is not modelled in 3-D, i.e. wrong measurement of the angle  $\beta$  see Figure 4.4b. On the other hand, the implicit IDA-PBC



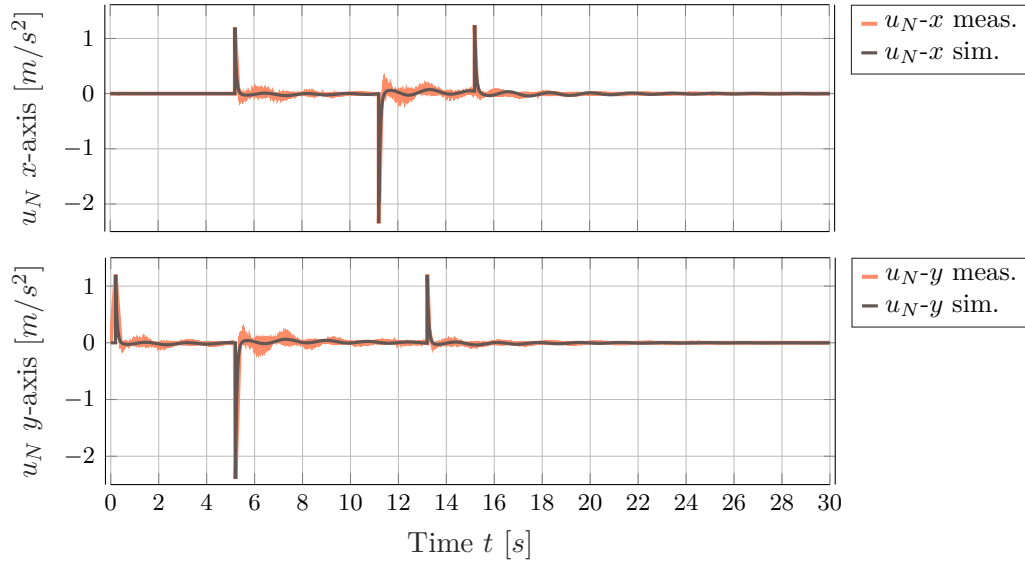


**Figure 4.20.** – Implicit control law output-feedback  $u_N$

approach has the advantage to have more tuning parameters, and the responses show less overshoot than the explicit method, a trade-off between doing it smoothly and doing it faster, with the selected values<sup>13</sup>.

Furthermore, it was possible to obtain an output-feedback law. Using this latter, we could appreciate a controller with less noise in the measurements, as show in a brief comparison between the control laws in Fig. (4.21). We can also appreciate that the measured pendulum positions  $x_p$ ,  $y_p$  and  $z_p$  have peaks of  $\approx 0.01m$ ,  $\approx 0.02m$  and  $\approx 0.9999m$  respectively for a state-feedback law, meanwhile that for an output-feedback law we can appreciate peaks of  $\approx 0.04m$ ,  $\approx 0.04m$  and  $\approx -0.9992m$ . Thus, we can appreciate more oscillations in  $x$ - and  $y$ -axis and an improvement in the  $z$ -axis by using the selected parameter in the output-feedback law. A brief comparison between the control laws is found in Fig. (4.21). Moreover, The computational algorithm has an improvement since we are not computing the velocities. To illustrate this latter, we show the performance measurement in Table 4.6 where the identification is developed in a computer with i5-4210H processor, 16 GB of RAM and MATLAB/Simulink in Windows 10.

<sup>13</sup>Let us remark that these values were the best the author of this thesis have found, however we do not claim that those are the best ones

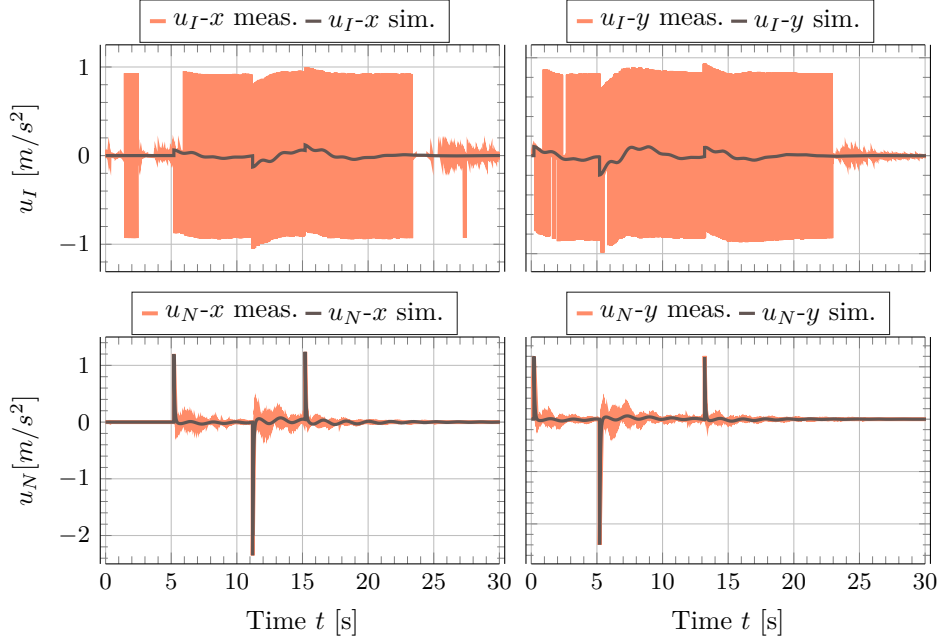


Figure 4.21. – Comparison between  $u_N$  and  $u_I$

Implicit IDA-PBC Technique	Solver	Sampling time [s]	Simulation time [s]	Computation time [s]
State-feedback	Runge-kutta ode4	0.001	36	14.2243
State-feedback	Runge-kutta ode4	0.01	36	3.1152
State-feedback	Domand-Prince ode8	0.001	36	35.4607
State-feedback	Domand-Prince ode8	0.01	36	4.4686
Output-feedback	Runge-kutta ode4	0.001	36	13.0429
Output-feedback	Runge-kutta ode4	0.01	36	2.9170
Output-feedback	Domand-Prince ode8	0.001	36	32.4135
Output-feedback	Domand-Prince ode8	0.01	36	5.6275

Table 4.6. – Performance Measurement

---

## Chapter 5

# Conclusions and Future Work

---

In this work, we put into practice a novel implicit IDA-PBC method developed by Cieza and Reger, where the total energy shaping is extended to underactuated mechanical systems modeled in implicit pH representation with the primary objective to avoid the persistent demand of solving PDEs in the classical (explicit) IDA-PBC. The first part of the thesis was devoted to showing that a mechanical system can be modeled in an explicit- or implicit-pH structure. Nevertheless, we witnessed that applying the IDA-PBC method might result in the presence of complex PDEs. Later, in Chapter 03, the propositions show an algebraic solution to achieve asymptotic stability (with IDA-PBC) avoiding PDEs in a class of systems modeled implicitly.

This thesis implements the total energy shaping explicit and implicit IDA-PBC techniques on a real portal crane system. However, in the first case, the model is restricted to 2-D (only one axis), and the solution of the matching conditions depends on a shrewd mathematical move. Simulations and experimentation show that the system in closed-loop is asymptotically stable, i.e., the standard IDA-PBC technique works. Despite the control law being designed only in the  $y$ -axis, we found that parallel application in the  $x$ -axis still achieves asymptotically stable results on the whole 3-D portal crane. In the second case, using the implicit IDA-PBC reduces the effort to design a suitable controller in the specific case of the portal crane; because, it fulfills the proposition conditions under simple algebra. Moreover, there is high flexibility in the tuning parameters, and the application of an output-feedback law was possible. In the simulations, the implicit IDA-PBC yields an asymptotically stable response for both cases, state- and output-feedback laws.

Synthesizing both approaches (implicit and explicit IDA-PBC) under partial feedback linearization results in controllers that are independent of the trolley and payload

mass, which are typically unknown or variable (in the payload case). Measured data in the implementation reflects a good behaviour of the system even though it was perturbed for parameters like vibration of the frame, friction, and lack of accuracy in the sensors. Lastly, this method validates the implicit IDA-PBC approach experimentally. Unfortunately, it was not possible to make an objective comparison between 2-D and 3-D IDA-PBC or even other controllers because a method that can contrast both with an appropriate reference parameters has not yet been defined and it goes beyond the scope of this thesis. Regardless of that, it shows a clear advantage in comparison with linear controllers from the perspective that is not limited to a specific operating point. However, the complexity of modeling the dynamics of a mechanical system in the implicit structure can be considered a trade-off.

Finally, it would be interesting if: (1) May be feasible to develop a technique which can serve as a tool for contrasting the implicit IDA-PBC with other controllers, perhaps through local linearization. (2) The implicit LMI approach presented in [43] can be implemented and compared with the results presented in this work. (3) Some uncertainties can be addressed, maybe through the extension of this work to sliding mode control or adaptive backstepping. (4) This method could be experimentally validated on non-holonomic systems, e.g. to a homogeneous ball on a rotating table.

# Appendices

---

## Appendix A

# Euler-Lagrange Equations

---

This Appendix is the demonstration of the Euler-Lagrange Equations. The demonstration is extracted from [23–25]

The well known Euler-Lagrange equations are a derivation from d’Alembert’s Principle. Equation (2.1) can be written such as the path followed by the system,

$$m_i \frac{d^2}{dt^2} \mathbf{r}_i - \mathbf{F}_i = 0. \quad (\text{A.1})$$

The virtual displacement  $\delta \mathbf{r}_i$  is a possible next infinitesimal part of the path, consistent with the constraints on the system,

$$\sum_i \left[ m_i \frac{d^2}{dt^2} \mathbf{r}_i - \mathbf{F}_i \right] \delta \mathbf{r}_i = 0. \quad (\text{A.2})$$

Equation (A.2) is well known as d’Alembert’s Principle, which is normally expressed as a scalar equation involving what is termed virtual work  $\mathbf{F}_i \delta \mathbf{r}_i$ , i.e. the work that would be done in the mass  $m_i$  in the virtual displacement  $\delta \mathbf{r}_i$ .

Then, using the virtual displacement Equation (2.5), Equation (A.2), becomes

$$\sum_{i,k} \left[ m_i \left( \ddot{\mathbf{r}}_i \frac{\partial \mathbf{r}_i}{\partial q_k} \right) - \left( \mathbf{F}_i \frac{\partial \mathbf{r}_i}{\partial q_k} \right) \right] \delta q_k = 0. \quad (\text{A.3})$$

Equation (A.3) is of the form

$$\sum_k \alpha_k \delta q_k = 0. \quad (\text{A.4})$$

Since the generalized coordinates  $\mathbf{q}$  are independent of one another, the  $\delta q_k$  are arbitrary. Therefore Equation (A.4) is valid if and only if each  $\alpha_k$  is independently zero for

each component  $k$ . Then,

$$\sum_{i=1}^n m_i \sum_{k=1}^{n_q} \left( \ddot{\mathbf{r}}_i \frac{\partial \mathbf{r}_i}{\partial q_k} \right) = \sum_{k=1}^{n_q} \left( \mathbf{F}^i \frac{\partial \mathbf{r}_i}{\partial q_k} \right). \quad (\text{A.5})$$

Because the Cartesian coordinates are functions of the generalized coordinates and the time, the time derivative of the coordinate  $\mathbf{r}_i$  is

$$\dot{\mathbf{r}}_i = \frac{d\mathbf{r}_i}{dt} = \sum_{k=1}^{n_q} \frac{\partial \mathbf{r}_i}{\partial q_k} \dot{q}_k + \frac{\partial \mathbf{r}_i}{\partial t} \quad (\text{A.6})$$

If we take the partial derivative of Equation (A.6) with respect to  $\dot{q}_k$  we will find what is often called *cancellation of the dots* because it appears as though we have simply cancelled the dots (time derivatives) in  $\partial \dot{\mathbf{r}}_i / \partial \dot{q}_k$  to obtain  $\partial \mathbf{r}_i / \partial q_k$ . Now, if we analyze the left part of Equation (A.5) we can notice that

$$\ddot{\mathbf{r}}_i \frac{\partial \mathbf{r}_i}{\partial q_k} = \ddot{\mathbf{r}}_i \frac{\partial \dot{\mathbf{r}}_i}{\partial \dot{q}_k} = \frac{d}{dt} \left( \dot{\mathbf{r}}_i \frac{\partial \dot{\mathbf{r}}_i}{\partial \dot{q}_k} \right) - \dot{\mathbf{r}}_i \frac{d}{dt} \left( \frac{\partial \dot{\mathbf{r}}_i}{\partial \dot{q}_k} \right). \quad (\text{A.7})$$

Since the partial derivative of  $\mathbf{r}_i$  with respect to generalized coordinates  $q_k$  depends on  $(q, t)$ , as does  $\dot{\mathbf{r}}_i$ , the time derivative of  $\partial \dot{\mathbf{r}}_i / \partial \dot{q}_k$  has the same form as Equation (A.6), that is

$$\frac{d}{dt} \left( \frac{\partial \dot{\mathbf{r}}_i}{\partial \dot{q}_k} \right) = \sum_{j=1}^{n_q} \frac{\partial^2 \dot{\mathbf{r}}_i}{\partial q_j \partial q_k} \dot{q}_j + \frac{\partial^2 \dot{\mathbf{r}}_i}{\partial t \partial q_k} \quad (\text{A.8})$$

where we can notice that Equation (A.6) appears in Equation (A.8)

$$\frac{d}{dt} \left( \frac{\partial \dot{\mathbf{r}}_i}{\partial \dot{q}_k} \right) = \frac{\partial}{\partial q_k} \underbrace{\left\{ \sum_{j=1}^{n_q} \frac{\partial \dot{\mathbf{r}}_i}{\partial q_j} \dot{q}_j + \frac{\partial \dot{\mathbf{r}}_i}{\partial t} \right\}}_{=\dot{\mathbf{r}}_i}.$$

Therefore,

$$\frac{d}{dt} \left( \frac{\partial \dot{\mathbf{r}}_i}{\partial \dot{q}_k} \right) = \frac{\partial \dot{\mathbf{r}}_i}{\partial q_k} \quad (\text{A.9})$$

Using Equation (A.9) in the right hand side of Equation (A.7)

$$\ddot{\mathbf{r}}_i \frac{\partial \mathbf{r}_i}{\partial q_k} = \frac{d}{dt} \left( \dot{\mathbf{r}}_i \frac{\partial \dot{\mathbf{r}}_i}{\partial \dot{q}_k} \right) - \dot{\mathbf{r}}_i \frac{\partial \dot{\mathbf{r}}_i}{\partial q_k} \quad (\text{A.10})$$

with

$$\dot{\mathbf{r}}_i \frac{\partial \dot{\mathbf{r}}_i}{\partial \dot{q}_k} = \frac{1}{2} \frac{\partial}{\partial \dot{q}_k} \dot{\mathbf{r}}_i^2 \quad \text{and} \quad \dot{\mathbf{r}}_i \frac{\partial \dot{\mathbf{r}}_i}{\partial q_k} = \frac{1}{2} \frac{\partial}{\partial q_k} \dot{\mathbf{r}}_i^2 \quad (\text{A.11})$$

we can arrange Equation (A.10) in

$$\ddot{\mathbf{r}}_i \frac{\partial \mathbf{r}_i}{\partial q_k} = \left[ \frac{d}{dt} \frac{\partial}{\partial \dot{q}_k} - \frac{\partial}{\partial q_k} \right] \left( \frac{1}{2} \dot{\mathbf{r}}_i^2 \right). \quad (\text{A.12})$$

Then using Equation (A.12), the left hand side of Equation (A.5) becomes

$$\begin{aligned} & \sum_{i=1}^n m_i \sum_{k=1}^{n_q} \left( \ddot{\mathbf{r}}_i \frac{\partial \mathbf{r}_i}{\partial q_k} \right) \\ &= \sum_{k=1}^{n_q} \left\{ \left[ \frac{d}{dt} \frac{\partial}{\partial \dot{q}_k} - \frac{\partial}{\partial q_k} \right] \sum_{i=1}^n m_i \left( \frac{1}{2} \dot{\mathbf{r}}_i^2 \right) \right\} \end{aligned} \quad (\text{A.13})$$

and from Equation (A.13) we recognize the kinetic energy, which we shall designate as

$$\begin{aligned} T &= \sum_i \frac{1}{2} m_i \dot{\mathbf{r}}_i^2 \\ &= \sum_i \frac{1}{2} m_i \mathbf{v}_i^2. \end{aligned} \quad (\text{A.14})$$

Equation (A.5) becomes

$$\sum_{k=1}^{n_q} \left[ \frac{d}{dt} \frac{\partial}{\partial \dot{q}_k} - \frac{\partial}{\partial q_k} \right] T = \sum_{k=1}^{n_q} \left( \mathbf{F}_i \frac{\partial \mathbf{r}_i}{\partial q_k} \right). \quad (\text{A.15})$$

We now recall that the remaining forces are conservative and are those arising from external fields. These forces are assumed to be equal to the negative gradient of a scalar called the potential Energy  $V$ , which is a function only of spatial coordinates. That is  $\mathbf{F}_i = -\partial V / \partial \mathbf{r}_i$ . Therefore, using the chain rule, becomes

$$\frac{\partial V}{\partial \mathbf{r}_i} \frac{\partial \mathbf{r}_i}{\partial q_k} = \frac{\partial V}{\partial q_k} \quad (\text{A.16})$$

since the potential energy  $V$  depends only on the coordinates and not on the velocities.

We also can notice that now

$$V\{\mathbf{r}_1, \mathbf{r}_2, \dots, \mathbf{r}_n\} \rightarrow V\{q_1, q_2, \dots, q_{n_q}\}. \quad (\text{A.17})$$

With Equation (A.16), Equation (A.15) becomes

$$\left[ \frac{\partial}{\partial q_k} - \frac{d}{dt} \frac{\partial}{\partial \dot{q}_k} \right] (T - V) = 0 \quad (\text{A.18})$$



Equation (A.18) are the *Euler-Lagrange* Equations. Meanwhile the combination of the Potential energy  $V$  and the Kinetic energy  $T$  is called the *Lagrangian*

$$L = T - V. \tag{A.19}$$

It is important to notice that the Lagrangian is a scalar function of the generalized coordinates  $\mathbf{q}$ , the time derivatives of the generalized coordinates  $\dot{\mathbf{q}}$ , and possibly the time  $t$ . To obtain the Lagrangian we only need the kinetic energies of the interacting bodies and the potential energies of the external fields (if they have a potential). Using the Lagrangian we obtain the final form of the Euler-Lagrange Equations

$$\frac{\partial L}{\partial q_k} - \frac{d}{dt} \left( \frac{\partial L}{\partial \dot{q}_k} \right) = 0. \tag{A.20}$$

---

## List of Acronyms

---

<b>PBC</b>	Passivity Based Control
<b>UMS</b>	Underactuated Mechanical System
<b>DOF</b>	Degrees of Freedom
<b>IDA-PBC</b>	Interconnection and Damping Assignment - Passivity-Based Control
<b>IDA</b>	Degrees of Freedom
<b>IDA</b>	Interconnection and Damping Assignment
<b>PFL</b>	Partial Feedback Linearization
<b>pH</b>	port-Hamiltonian
<b>PDE</b>	Partial Differential Equation
<b>IDE</b>	Integral Dissipation Inequality
<b>DDI</b>	Differential Dissipativity Inequality
<b>DAE</b>	Differential-Algebraic Equation

---

## List of Figures

---

1.1. Different kind of cranes . . . . .	3
2.1. Rectangular Cartesian Coordinates . . . . .	9
2.2. Pendulum with generalized coordinate $\beta$ . . . . .	9
3.1. Algorithm for the algebraic implicit IDA-PBC . . . . .	31
4.1. Subfigures showing the portal crane system at the laboratory. . . . .	35
4.2. Sketch of the portal crane. . . . .	35
4.3. Trolley and its elements . . . . .	36
4.4. Subfigures showing the relationship between the angles and the general- ized coordinates . . . . .	37
4.5. PC, dSPACE and Portal Crane . . . . .	37
4.6. 2-D crane . . . . .	38
4.7. Subfigures showing the portal crane 3-D model . . . . .	40
4.8. (Explicit) IDA-PBC block diagram . . . . .	46
4.9. Block crane plus partial feedback linearization (CRANE + PFL) . . . . .	46
4.10. Simulated and measured trolley displacement in $y$ -axis . . . . .	47
4.11. Simulated and measured swing angle $\alpha$ in the $y$ -axis. Note that is as- sumed that $\beta \equiv 0$ . . . . .	47
4.12. Simulated (Explicit) IDA-PBC control law $u_{IDA}$ applied in the $y$ -direction and the measured control law . . . . .	47
4.13. Implicit algebraic IDA-PBC block diagram . . . . .	50
4.14. Simulation with state-feedback law $u_I$ for desire $x_c$ and $y_c$ . . . . .	51
4.15. Implementation implicit IDA-PBC and response of $\mathbf{r}$ . . . . .	52
4.16. Implicit control law $u_I$ . . . . .	53
4.17. Implicit Output-feedback IDA-PBC applied to the Portal Crane Block Diagram . . . . .	53
4.18. Implicit Output-feedback IDA-PBC controller diagram . . . . .	53

**LIST OF FIGURES**

---

4.19. Output-feedback measurement . . . . .	54
4.20. Implicit control law output-feedback $u_N$ . . . . .	55
4.21. Comparison between $u_N$ and $u_I$ . . . . .	56

---

## List of Tables

---

2.1. Types of passivity . . . . .	16
4.1. Controller Board Specifications . . . . .	38
4.2. Crane constant parameters . . . . .	45
4.3. (Explicit) IDA-PBC tuning paramaters . . . . .	46
4.4. Parameters for implicit state feedback IDA-PBC . . . . .	49
4.5. Parameters for implicit output-feedback IDA-PBC . . . . .	50
4.6. Performance Measurement . . . . .	56

---

## Bibliography

---

- [1] L. Xue and G. Zhiyong, “Control of underactuated bridge cranes: A simplified ida-pbc approach,” in *11th Asian Control Conference (ASCC)*, 2017, pp. 717–722.
- [2] M. W. Spong, “Underactuated mechanical systems,” in *Control problems in robotics and automation*. Springer, 1998, pp. 135–150.
- [3] A. Macchelli, “Passivity-based control of implicit port-Hamiltonian systems,” *SIAM Journal on Control and Optimization*, vol. 52, no. 4, pp. 2422–2448, 2014.
- [4] O. Cieza Aguirre and J. Reger, “IDA-PBC for underactuated mechanical systems in implicit port-hamiltonian representation,” *European Control Conference (ECC) 2019*, pp. 614–619.
- [5] Siemens. Heavy lifting in the industry. [Online]. Available: <https://new.siemens.com/global/en/markets/cranes/industry-cranes.html>
- [6] E. M. Abdel-Rahman, A. H. Nayfeh, and Z. N. Masoud, “Dynamics and control of cranes: A review,” *Modal Analysis*, vol. 9, no. 7, pp. 863–908, 2003.
- [7] M. cranes, “Portain mdt 98 data sheet.” [Online]. Available: [www.manitowoc.com](http://www.manitowoc.com)
- [8] Ale. The latest crane lifting technology for any project challenge. [Online]. Available: <https://www.ale-heavylift.com/services/heavy-crane-lifting/>
- [9] L. Aimix Group Co. Rubber-Tyred gantry crane Terex. [Online]. Available: <https://gantrycranesmanufacturer.com/rubber-tyred-gantry-crane/>
- [10] B. d’Andréa Novel, F. Boustany, F. Conrad, and B. Rao, “Feedback stabilization of a hybrid PDE-ODE system: Application to an overhead crane,” *Mathematics of Control, Signals and Systems*, vol. 7, no. 1, pp. 1–22, 1994.
- [11] N. B. Almutairi and M. Zribi, “Sliding mode control of a three-dimensional overhead crane,” *Journal of vibration and control*, vol. 15, no. 11, pp. 1679–1730, 2009.

- [12] C. Vázquez, L. Fridman, J. Collado, and I. Castillo, “Second-order sliding mode control of a perturbed-crane,” *Journal of Dynamic Systems, Measurement, and Control*, vol. 137, no. 8, 2015.
- [13] X. Weimin, Z. Xiang, L. Yuqiang, Z. Mengjie, and L. Yuyang, “Adaptive dynamic sliding mode control for overhead cranes,” in *2015 34th Chinese Control Conference (CCC)*. IEEE, 2015, pp. 3287–3292.
- [14] J. L. Zarate Moya, “Tracking controller design for a nonlinear model of a gantry crane based on dynamic extension and robustification,” mathesis, Technische Universität Ilmenau, 2015.
- [15] R. Banavar, F. Kazi, R. Ortega, and N. Manjarekar, “The IDA-PBC methodology applied to a gantry crane,” in *Proceedings of the Mathematical Theory of Networks and Systems*. Kyoto, Japan, 2006, pp. 143–147.
- [16] M. Ryalat and D. S. Laila, “A simplified IDA-PBC design for underactuated mechanical systems with applications,” *European Journal of Control*, vol. 27, pp. 1–16, 2016.
- [17] F. Kazi, R. Banavar, R. Ortega, and N. Manjarekar, “Point-to-point control of a gantry crane: A combined flatness and ida-pbc strategy,” in *European Control Conference (ECC)*, 2007, pp. 5815–5820.
- [18] A. Donaire, R. Mehra, R. Ortega, S. Satpute, J. G. Romero, F. Kazi, and N. M. Singh, “Shaping the energy of mechanical systems without solving partial differential equations,” in *2015 American Control Conference (ACC)*. IEEE, 2015, pp. 1351–1356.
- [19] R. Mehra, S. Satpute, F. Kazi, and N. Singh, “Geometric-PBC based control of 4-dof underactuated overhead crane system,” in *International Symposium on Mathematical Theory of Networks and Systems*, 2014, pp. 1232–1237.
- [20] W. R. Hamilton, *The Mathematical Papers of Sir William Rowan Hamilton*. CUP Archive, 1931, vol. 2.
- [21] C. Lanczos, *The variational principles of mechanics*. Courier Corporation, 2012.
- [22] F. Castaños, D. Gromov, V. Hayward, and H. Michalska, “Implicit and explicit representations of continuous-time port-Hamiltonian systems,” *Systems & Control Letters*, vol. 62, no. 4, pp. 324–330, Apr. 2013.
- [23] C. S. Helrich, *Analytical Mechanics*. Springer International Publishing, 2017.

- [24] L. N. Hand and J. D. Finch, *Analytical mechanics*. Cambridge University Press, 1998.
- [25] V. Arnold, *Mathematical methods of classical mechanics*, second edition ed. Springer, 1989.
- [26] J. L. Meriam, L. G. Kraige, and B. J. N, *Engineering mechanics: dynamics*. John Wiley & Sons, 2015, vol. 2.
- [27] K. Andreas, *Mathematical Physics: Classical Mechanics*. Springer, 2018.
- [28] R. Ortega and M. W. Spong, “Adaptive motion control of rigid robots: A tutorial,” *Automatica*, vol. 25, no. 6, pp. 877–888, 1989.
- [29] M. Takegaki and S. Arimoto, “A new feedback method for dynamic control of manipulators,” *Journal of Dynamic Systems, Measurement, and Control*, vol. 103, no. 2, pp. 119–125, 1981.
- [30] S. Delgado, “Total energy shaping for Underactuated Mechanical Systems: Dissipation and nonholonomic constraints,” PhD Thesis, Technische Universität München, 2016.
- [31] R. Ortega, J. A. L. Perez, P. J. Nicklasson, and H. J. Sira-Ramirez, *Passivity-based control of Euler-Lagrange systems: mechanical, electrical and electromechanical applications*. Springer, 2013.
- [32] A. J. van der Schaft and A. Van Der Schaft, *L2-gain and passivity techniques in nonlinear control*. Springer, 2000.
- [33] R. Sepulchre, M. Jankovic, and P. V. Kokotovic, *Constructive nonlinear control*. Springer Science, 2012.
- [34] A. Astolfi, R. Ortega, and R. Sepulchre, “Stabilization and disturbance attenuation of nonlinear systems using dissipativity theory,” *European journal of control*, vol. 8, no. 5, pp. 408–431, 2002.
- [35] C. I. Byrnes, A. Isidori, and J. C. Willems, “Passivity, feedback equivalence, and the global stabilization of minimum phase nonlinear systems,” *IEEE Transactions on automatic control*, vol. 36, no. 11, pp. 1228–1240, 1991.
- [36] J. A. Popayán, O. B. Cieza, and J. Reger, “Adaptive ida-abc for a class of umss: The iwip analysis,” *IFAC Symposium on Nonlinear Control Systems (NOLCOS)*, 2019.



- [37] A. Ilchmann and T. Reis, “Surveys in Differential-Algebraic Equations i,” A. van der Schaft, Ed. Springer, 2013, vol. I, ch. Port-Hamiltonian Differential-Algebraic Systems, pp. 173–224.
- [38] V. Duindam, A. Macchelli, S. Stramigioli, and H. Bruyninckx, *Modeling and Control of Complex Physical Systems: The Port Hamiltonian Approach*. Springer, 2009.
- [39] F. Castaños and D. Gromov, “Passivity-based control of implicit port-Hamiltonian systems with holonomic constraints,” *Systems & Control Letters*, vol. 94, pp. 11–18, 2016.
- [40] R. Ortega, A. Van Der Schaft, B. Maschke, and G. Escobar, “Interconnection and damping assignment passivity-based control of port-controlled Hamiltonian systems,” *Automatica*, vol. 38, no. 4, pp. 585–596, 2002.
- [41] R. Ortega, A. Van der Schaft, B. Maschke, and G. Escobar, “Energy-shaping of port-controlled Hamiltonian systems by interconnection,” in *Conference on Decision and Control (CDC)*, 1999, pp. 1646–1651.
- [42] R. Ortega, M. W. Spong, F. Gómez-Estern, and G. Blankenstein, “Stabilization of a class of underactuated mechanical systems via interconnection and damping assignment,” *IEEE transactions on automatic control*, vol. 47, no. 8, pp. 1218–1233, 2002.
- [43] O. Cieza Aguirre and J. Reger, “Implicit IDA-PBC for underactuated mechanical systems: An lmi-based approach,” 2019, accepted for the Conference on Decision and Control - (CDC 2019).
- [44] D. P. Bertsekas, *Constrained optimization and Lagrange multiplier methods*. Academic press, 1996.
- [45] Z. Zhang, Y. Wu, and J. Huang, “Differential-flatness-based finite-time anti-swing control of underactuated crane systems,” *Nonlinear Dynamics*, vol. 87, no. 3, pp. 1749–1761, 2017.
- [46] R. Singhal, R. Patayane, and R. N. Banavar, “Tracking a trajectory for a gantry crane: Comparison between ida-pbc and direct lyapunov approach,” in *International Conference on Industrial Technology*, 2006, pp. 1788–1793.
- [47] X. Wu and X. He, “Partial feedback linearization control for 3-d underactuated overhead crane systems,” *ISA transactions*, vol. 65, pp. 361–370, 2016.

- [48] “dSPACE company website.” [Online]. Available: <https://www.dspace.com/de/gmb/home.cfm>
- [49] M. W. Spong, “Partial feedback linearization of underactuated mechanical systems,” in *International Conference on Intelligent Robots and Systems (IROS)*, 1994, pp. 314–321.
- [50] N. Sun and Y. Fang, “An efficient online trajectory generating method for underactuated crane systems,” *International Journal of Robust and Nonlinear Control*, vol. 24, no. 11, pp. 1653–1663, 2014.